Title

Recognition of microbe/damage-associated molecular patterns by leucine-rich repeat pattern recognition receptor kinases confers salt tolerance in plants

Authors

Eliza P-I. Loo[1,a,**], Yuri Tajima[1,b,**], Kohji Yamada[2,c], Shota Kido[1], Taishi Hirase[1,d], Hirotaka Ariga[3,e], Tadashi Fujiwara[1], Keisuke Tanaka[4], Teruaki Taji[3], Imre E. Somssich[2], Jane E. Parker[2,5] and Yusuke Saijo[1,2,6*]

[1]Graduate School of Biological Sciences, Nara Institute of Science and Technology, Ikoma, 630-0192 Japan

[2]Department of Plant Microbe Interactions, Max Planck Institute for Plant Breeding Research, Cologne, 50829 Germany

[3]Department of Bioscience, Tokyo University of Agriculture, Tokyo, 156-8502 Japan

[4]NODAI Genome Research Center, Tokyo University of Agriculture, Tokyo, 156-8502 Japan

[5]Cologne-Düsseldorf Cluster of Excellence on Plant Sciences (CEPLAS), 40225 Germany

[6]JST PRESTO, Kawaguchi, 332-0012 Japan

[a] Present address: Institute for Molecular Physiology, Heinrich-Heine-Universität, 40225 Germany

[b] Present address: Faculty of Life and Environmental Sciences, University of Tsukuba, Tsukuba, Ibaraki, 305-8572 Japan

[c] Present address: Graduate School of Technology, Industrial and Social Sciences, Tokushima University, Tokushima, 770-8501 Japan

[d] Present address: Leaf Tobacco Research Center, JAPAN TOBACCO Inc, Oyama, 323-0808 Japan

[e] Present address: Genetic Resources Center, NARO, Ibaraki, 305-8602 Japan

*Corresponding author: saijo@bs.naist.jp

** These authors contributed equally to this work.

Keywords: pattern recognition receptor, plant immunity, biotic-abiotic stress, plant-microbe-environment interactions, salt stress tolerance

Funding: This work was supported in part by the grants from the MEXT of Japan (no. 18H04783, 18H02467 and 21H02507 to Y.S., 19H03092 to T.T.), grants from SFB670 (Y.S., I.S., J.P.), JST PRESTO (Y.S.), the Asahi Glass Foundation (T.T.) and the Max Planck Society (Y.S., I.S., J.P.), and PhD fellowships from the Japanese Government Scholarship for International Priority Programs (E.L.) and from the Japan Society for the Promotion of Science (T.H.).

Abstract

In plants, a first layer of inducible immunity is conferred by pattern recognition receptors (PRRs) that bind microbe- and damage-associated molecular patterns (MAMPs/DAMPs, respectively) to activate pattern-triggered immunity (PTI). PTI is strengthened or followed by another potent form of immunity when intracellular receptors recognize pathogen effectors, termed effector-triggered immunity (ETI). Immunity signaling regulators have been reported to influence abiotic stress responses as well, yet the governing principles and mechanisms remain ambiguous. Here, we report that PRRs of a leucine-rich repeat ectodomain also confer salt tolerance in *Arabidopsis thaliana*, following recognition of cognate ligands, such as bacterial flagellin (flg22 epitope) and EF-Tu (elf18 epitope), and the endogenous Pep peptides. Pattern-triggered salt tolerance (PTST) requires authentic PTI signaling components, namely the PRR-associated kinases *BAK1* and *BIK1*, and the NADPH oxidase *RBOHD*. Exposure to salt stress induces the release of Pep precursors, pointing to the involvement of the endogenous immunogenic peptides in developing plant tolerance to high salinity. Transcriptome profiling reveals an inventory of PTST target genes, which increase or acquire salt responsiveness following a pre-exposure to immunogenic patterns. In good accordance, plants challenged with non-pathogenic bacteria also acquired salt tolerance in a manner dependent on PRRs. Our findings provide insight into signaling plasticity underlying biotic-abiotic stress cross-tolerance in plants conferred by PRRs.

INTRODUCTION

Like animals, plants have evolved an elaborate immune system to sense and adapt to disturbance caused by biotic agents. How the immune system influences abiotic stress responses remains much less understood. Plants sense and cope with fluctuating environments, while accommodating a rich diversity of microbial communities that often aid host adaptation. Conversely, environmental abiotic factors, such as light, temperature and water availability profoundly influence the mode and outcome of plant-microbe interactions (Velásquez et al. 2018). This predicts an intimate relationship between biotic and abiotic stress sensing and signaling in plants. In line with this, it is becoming apparent that immune receptors and signaling regulators also impact abiotic stress responses, positively or negatively in a context-dependent manner (Saijo and Loo 2020). However, the regulatory logic or molecular basis behind intricate cross-regulations between biotic and abiotic stress signaling remains poorly understood.

Plant immunity largely relies on two classes of innate immune receptors, namely cell surface-localized PRRs and intracellular nucleotide-binding domain and leucine-rich repeat (LRR)-containing receptors (NLRs) (Jones and Dangl 2006). Detection of MAMPs and DAMPs by cognate PRRs leads to pattern-triggered immunity (PTI), which is vital in preventing the infection of most non-adapted microbes and in restricting growth of adapted microbes, termed basal resistance (DeFalco and Zipfel 2021; Saijo et al. 2018). In turn, plant-infecting microbes, whether pathogenic or non-pathogenic, employ an array of effectors to manipulate host immunity and other processes for infection. To counter this, plants employ a repertoire of NLRs that recognize microbial effectors to mount effector-triggered immunity (ETI) that terminates microbial growth. NLRs are

classified into two major subclasses, based on their N-terminal domains: the coiled-coil (CC)-NLRs and the Toll-interleukin1-receptor (TIR)-NLRs. CC-NLR and TIR-NLR functions typically require the defense regulators *NDR1* and *EDS1*, respectively (Jones *et al*, 2016). Compared to PTI, ETI is typically greater in amplitude and robustness against microbial perturbations, and is often accompanied by localized cell death called the hypersensitive response (Cui et al. 2015). Molecular genetic studies in *Arabidopsis thaliana* interactions with the bacterial pathogen *Pseudomonas syringae* pv *tomato* DC3000 (*Pst*) indicate mutual inter-dependence between PTI and ETI (Ngou et al. 2021; Yuan et al. 2021).

A major class of PRRs are the LRR-receptor kinases (RKs), including FLS2, EFR and PEPR1/PEPR2, which recognize bacterial flagellin (flg22 epitope), elongation factor Tu (EF-Tu, elf18 epitope) and the endogenous Pep epitopes embedded in their precursors, PROPEPs, respectively (Gómez‐Gómez and Boller 2000; Zipfel et al. 2006; Yamaguchi et al. 2006, 2010; Krol et al. 2010). Following ligand binding, these PRRs form heteromeric receptor complexes with the LRR-RK BAK1 (and related SERKs), and then induce dissociation of receptor-like cytoplasmic kinases (RLCKs) such as BIK1 and PBL1. Their trans-phosphorylation provides a basis for intracellular defense signaling, which involves Ca^{2+} release and an RBOHD-dependent reactive oxygen species (ROS) burst, phosphorylation cascades of Ca^{2+}-dependent protein kinases and mitogen-activated protein kinases (MAPKs), callose deposition, production of the phytohormones ethylene and salicylic acid (SA), and extensive reprogramming of the transcriptome and proteome (Couto & Zipfel, 2016; Yu *et al*, 2017; Saijo *et al*, 2018). These signaling events collectively contribute to

PTI, and also provide possible internodes for balancing immunity and other cellular processes.

Activation of PTI is required to potentiate ETI for effective pathogen resistance (Ngou et al. 2021; Yuan et al. 2021). SA is a key for this process in biotrophic/hemibiotrophic pathogen resistance, and is produced in large part through the SA biosynthetic enzyme isochorismate synthase1 (ICS1) during PTI (Wildermuth et al. 2001; Vlot et al. 2009). SA signaling relies on the SA-binding transcriptional co-activator *NPR1* and co-repressors *NPR3/NPR4* (Ding and Ding 2020), and also on *EDS1* and related *PAD4* (Wiermer et al. 2005). *EDS1/PAD4* activate *ICS1* expression and SA accumulation but also promote *ICS1*/SA-independent defenses (Glazebeook et al. 2003; Bartsch et al. 2006; Cui et al. 2017). Accordingly, *EDS1* is required for basal resistance to biotrophic and hemi-biotrophic pathogens (Dongus and Parker 2021). However, excessive de-repression of *EDS1/PAD4*-mediated defenses during osmotic stress results in a collapse of osmotic stress tolerance (Ariga et al. 2017). Therefore, tight control of EDS1/PAD4 activity is crucial not only under biotic but also abiotic stress conditions.

Genetic studies have implicated PRRs in salt stress tolerance. In *Arabidopsis thaliana*, ectopic expression of fungal chitinase or chitin application enhances salt tolerance in a manner dependent on the lysin-motif (LysM) RK *CERK1*, which mediates the perception of fungal chitin and bacterial peptidoglycans (Brotman et al. 2012). Even under sterile conditions in the absence of microbes or MAMPs, *cerk1* plants are hypersensitive to salt stress (Espinoza et al. 2017). These studies suggest that *CERK1* has a role in promoting salt stress tolerance, and that this function is related to an as-yet-unidentified endogenous DAMP(s). Likewise, *PROPEP3* overexpression and

Pep3 application under sterile conditions both enhance salt tolerance through *PEPR1* (Nakaminami et al. 2018). These studies suggest that DAMP sensing and signaling contribute to salt stress tolerance, yet the underling principles are not defined.

Here, we report that PTI signaling components promote salt tolerance in *A. thaliana* following recognition of various immunogenic patterns. Transcriptome profiling reveals an inventory of defense/stress-related genes that increase or acquire salt responsiveness after PRR elicitation. Recognition of non-pathogenic bacteria also leads to salt tolerance through these PRR signaling components. Our findings indicate that immunogenic pattern sensing of cellular damage and plant-associated microbes is intimately linked to salt stress tolerance.

RESULTS

Recognition of damage/microbe-associated molecular patterns leads to salt tolerance

Whole-genome microarray analysis for Pep2- and elf18-induced transcriptional reprogramming in *Arabidopsis* seedlings (Ross et al. 2014) produced an inventory of Pep2- and elf18-inducible genes (≧4-fold), i.e. 575 and 76 genes with Pep2 at 2 h and 10 h, respectively, and 536 and 380 genes with elf18 at 2 h and 10 h, respectively. *In silico* data analysis suggests that the majority of these PTI-inducible genes are also induced in seedling shoots or roots in response to salt and osmotic stresses (Supplementary Fig. S1A), as previously described for chitin (Espinoza et al. 2017). The common target genes included members of the *PROPEP* family and *PEPR1/PEPR2* (Supplementary Fig. S1A), implying the extensive engagement of this DAMP

pathway under salt stress. These data prompted us to examine whether recognition of different MAMPs and DAMPs leads to salt stress tolerance, and if so, by what mechanism.

We first tested whether pretreatment of seedlings with Pep, flg22 and elf18 peptides confers salt stress tolerance. Salt tolerance was determined as the ratio of viable (green) plants to dead/dying plants with bleached leaves, over the total number of the tested plants (Fig. 1A, Fig. 3A). In non-elicited plants, the survival rate declined to 36%, while survival of Pep1-pretreated seedlings was 94%, 7 d after salt stress (Fig. 1B). Pep1-triggered salt stress was effective, at least up to 200 mM NaCl (Supplementary Fig. S1B). Pep1, Pep2, Pep3 and Pep4 pretreatments all significantly increased plant tolerance to 175 mM NaCl (Supplementary Fig. S1C, Table 1). Pep1 pretreatment resulted in increases in overall seedling fresh weight and chlorophyll contents (Fig. 1C-D), pointing to enhanced salt stress tolerance (Acosta-Motos et al. 2017). PEPR1 recognizes all Pep peptides while PEPR2 recognizes only Pep1 and Pep2 (Krol et al. 2010; Bartels et al. 2013). Although it was previously described that *PEPR1*, but not *PEPR2*, is required for Pep3-triggered salt tolerance (Nakaminami et al. 2018), our analysis showed that Pep1-triggered salt tolerance was retained in *pepr1* or *pepr2* but abolished in *pepr1 pepr2* plants (Fig. 1, Table 1). Accordingly, Pep1 effects on shoot fresh weights and chlorophyll contents under salt stress was absent in *pepr1 pepr2* plants (Fig. 1C-D). The results indicate that PEPR1 and PEPR2 both mediate salt tolerance, despite their differences in Pep ligand specificity.

PRR signaling activation under sterile conditions typically leads to growth retardation (Boller and Felix 2009). Conceivably, the lowered metabolic activity accompanying reduced growth could lower salt uptake into the plant, thereby

conferring apparent tolerance. However, *pepr2* plants acquired salt tolerance following Pep1 application (Table 1), without discernible growth inhibition (Krol et al. 2010). Pep3 and Pep4 application also conferred salt tolerance without significantly inhibiting root growth (Supplementary Fig. S1C, Table 1). This indicates that plant growth inhibition is not required for pattern-triggered salt tolerance, which we designate as PTST.

Importantly, pretreatment with flg22 or elf18 also conferred salt tolerance through cognate PRRs (Fig. 1E-F, Supplementary Fig. S1D). The results indicate that PTST is not specific to an immunogenic pattern or receptor but is common to a broad range of MAMPs/DAMPs. This is consistent with the view established in plant immunity that a wide array of PRRs link the recognition of diverse cognate ligands to a largely overlapping set of defense outputs (Saijo et al, 2018). The ligand dose dependence of flg22-induced salt tolerance was comparable with that of other flg22-induced outputs (Supplementary Fig. S1D) (Gómez-Gómez et al. 1999; Aslam et al. 2009). These results suggest that PTST shares post-recognition signaling mechanisms with PTI across different PRR pathways. Notably, chitin application did not affect salt tolerance under our conditions, despite significant induction of a defense marker, *CYP71A13*, encoding cytochrome P450 involved in camalexin biosynthesis (Supplementary Fig. S1E).

Pattern-triggered salt tolerance and pattern-triggered immunity share early signaling steps downstream of the receptor

A major branch of PTI signaling triggered by the LRR-domain PRRs occurs through the receptor complexes with BAK1 and BIK1/PBL1 ((Couto and Zipfel 2016). To test possible *BAK1* dependence of PTST, we examined Pep1-

triggered salt tolerance in a null *bak1-4* allele, and a hypoactive *bak1-5* allele specifically impaired in PRR-related BAK1 function (Roux et al. 2011; Schwessinger et al. 2011). We previously described retention of PEPR-mediated defenses in *bak1* null mutants, reflecting PEPR1 interactions with other BAK1-related RKs (Yamada et al. 2016). Consistently, Pep1-induced salt tolerance was unaffected in *bak1-4* (Fig. 2). However, it was severely compromised in *bak1-5* plants and *bak1-5 bkk1* plants that additionally lack BAK1-related RK *BKK1*, required for PEPR-mediated defenses (Yamada et al. 2016) (Fig. 2). Likewise, Pep1-induced salt tolerance was also impaired in *bik1 pbl1* plants (Fig. 2). The results indicate that PTST signaling also occurs through these BAK1-related RKs and RLCKs.

Interestingly, seedling survival rate was also significantly lowered in *bak1-5*, *bak1-5 bkk1,* and *bik1 pbl1* plants when exposed to salt stress without exogenous Pep1 pretreatment (Fig. 2, mock controls), pointing to engagement of these PRR-associated kinases in salt tolerance. Our data suggest that the authentic receptor complexes mediate PTST, and that DAMPs or endogenous ligands generated under salt stress signal via *BAK1/BIK1*-dependent PRRs or receptors.

Pep1-triggered salt tolerance was reduced in *rbohd* plants lacking the PRR-associated NADPH oxidase responsible for a pattern-induced ROS burst (Fig. 2; Kadota *et al*, 2015), pointing to a critical role also for this PRR output in PTST. By contrast, callose synthase *PMR4/GSL5* mediating callose deposition during PTI (Kim et al. 2005) was not required for Pep1-triggered salt tolerance (Fig. 2), demonstrating that PRR-induced callose deposition is dispensable for PTST.

FLS2-mediated salt tolerance was also reduced in *bak1-5* plants, indicated by decreases in the survival rate, seedling fresh weight and chlorophyll contents under salt stress after flg22 pretreatment (Fig. 3A-C). It was also reduced in *bak1-4* plants, indicated by chlorophyll contents (Fig. 3C), although the survival rate or seedling fresh weight was not significantly reduced (Fig 3A-B). The partial retention of PTST may be attributed to a *BAK1*-independent pathway mobilized by residual FLS2 signaling in the mutant. Nevertheless, the results indicate that PTST through these LRR-RKs relies on PRR-regulating *BAK1* function, and that early signaling steps within and proximal to the PRR complexes, if not all, are shared between PTI and PTST.

Pattern-triggered salt tolerance is robust against hormone perturbations

PRR signaling involves complex networks of defense-related hormones including SA, JA and ethylene in PTI (Pieterse et al. 2012). FLS2- and EFR-triggered immunity largely collapses in the simultaneous absence of *DDE2* encoding allene oxide synthase (AOS) required for JA biosynthesis, *EIN2* encoding the master regulator of ethylene signaling, *SID2* (*ICS1*) and *PAD4* (Tsuda et al. 2009). However, in *dde2 ein2 pad4 sid2* plants, PTST was unaffected (Supplementary Fig. S2A), indicating that these defense-related sectors are all dispensable for PTST.

We also assessed whether PTST is dependent on ABA, which is central to plant adaptation to salt, osmotic and water-deficit stresses (Cutler et al. 2010; Finkelstein 2013). PTST was unaffected in *aba2-12* plants impaired in ABA biosynthesis (González-Guzmán et al. 2002) and in *areb1 areb2 abf3* plants lacking key transcription factors mediating ABA responses (Yoshida et al. 2015) (Supplementary Figs. S2B and S2C), suggesting that ABA is also dispensable

for PTST. Overall, our findings point to high PTST robustness against perturbations of these biotic/abiotic stress-related hormone pathways.

Salt-induced damage sensing and signaling involves the Pep-PEPR pathway

To test involvement of endogenous DAMPs in salt tolerance, we monitored endogenous PROPEP-PEPR signaling under salt stress. Given the substantial induction of *PROPEPs* and *PEPR1/PEPR2* in roots (Supplementary Fig. S1A), we examined PROPEP3 protein expression in the roots of transgenic plants expressing *PROPEP3-Venus* under its native regulatory DNA sequences. A strong PROPEP3-Venus fluorescence signal was detected 24 h after salt stress, but not under mock conditions (Fig. 4A). Damage-induced release of PROPEP1 from the vacuole and that of PROPEP3 to extracellular spaces (Hander et al. 2019; Yamada et al. 2016) prompted us to test for possible PROPEP release under salt stress. We traced PROPEP3-Venus accumulation in the surrounding liquid media, following salt stress and/or Pep1 application. Immunoblot analysis with PROPEP3-specific antibodies (Ross et al. 2014) detected specific signals that were close to the predicted full-length size of PROPEP3-Venus (~10.4 + 27 kDa) (Yamada et al. 2016) following Pep1 application (Fig. 4B), as described for Pep2 application (Yamada et al. 2016). Apparently shorter forms of PROPEP3-Venus were additionally detected under salt stress with or without Pep1 application (Fig. 4B), possibly reflecting PROPEP3 processing that may occur in the intracellular or extracellular spaces. Under these conditions, endogenous PROPEP3-derived signals were not detected. Nevertheless, these results validate that PROPEP3 is released under salt stress.

To assess a possible contribution of the endogenous PEPR pathway to salt tolerance, we examined salt responses of PEPR1 and PEPR2 over-expressing lines (*PEPR1-OE* or *PEPR2-OE,* respectively) in the *pepr1 pepr2* background, without exogenous application of Peps or MAMPs. *PEPR1-OE* and *PEPR2-OE* plants both exhibited increased survival rates when exposed to 175 mM NaCl compared to that of *pepr1 pepr2* plants (Fig. 4C). Moreover, following 7-d acclimatization to mild salt stress (100 mM NaCl), *PEPR1-OE* and *PEPR2-OE* plants acquired enhanced tolerance to severe osmotic stress (750 mM sorbitol) compared to *pepr1 pepr2* plants, indicated by the leaf chlorophyll contents (Fig. 4D). These data provide compelling evidence that an endogenous PEPR pathway contributes to salt and osmotic stress tolerance, in the absence of exogenous Pep application. Collectively, the results indicate that salt stress induces the generation and release of PROPEP-derived peptides, which engages PEPR signaling in salt/osmotic stress tolerance.

Pep1 pretreatment strengthens transcriptome dynamics in response to salt stress

To gain a mechanistic insight into PTST, we performed transcriptome profiling on WT and *pepr1 pepr2* plants during the course of PTST. To capture useful information from the salt-sensitive samples, plants were subjected to 150 mM NaCl after Pep1 application. As salt-induced transcriptional reprogramming is largely achieved within the first 24 h (Geng et al. 2013), we obtained the data under salt stress for 3 h and 24 h, after a 3-d Pep1 pretreatment (Fig. 5A). Up- or down-regulated genes under salt stress in non-elicited plants (mock), with a cut-off of $|\log_2 (\text{fold change})| \geqq 1$ ($p < 0.05$), were assembled at the indicated times, defining the salt-responsive differentially expressed genes (DEGs) (Fig.

5B). Likewise, genes whose expression was significantly altered, both between Pep1- and mock-pretreated WT plants and between Pep1-pretreated WT plants and *pepr1 pepr2* plants, were assembled at the indicated times under salt stress, defining PTST-DEGs (exhibiting Pep1/*PEPR*-dependent alterations in salt responsiveness) (Fig. 5B). DEGs were scored at the earliest time points when their expression levels first met these criteria.

In non-elicited plants under salt stress, we detected a total of 1,285 up- vs. 911 down-regulated DEGs, and 1,497 up- vs. 1,363 down-regulated DEGs, at 3h and 24 h, respectively (Fig. 5B). This suggests that salt-induced transcriptional reprogramming persisted over the tested time window. In Pep1-pretreated plants, we detected 639 up- vs. 416 down-regulated PTST-DEGs 3 h after salt stress, but merely 32 up- vs. 315 down-regulated PTST-DEGs at 24 h (Fig. 5B). This suggests that PRR signaling particularly impacts the early responsiveness of salt-inducible genes.

Next, we examined possible overlap and divergence between the obtained salt-inducible DEGs and the previously described, Pep2- or elf18-responsive DEGs (2 h and 10 h; Ross *et al*, 2014). This showed that 599 genes (34.1% of Pep2/elf18-inducible genes and 22.9% of salt-inducible genes) were commonly induced between the two types of stimuli, while 1,155 and 2,012 genes were specifically induced in response to Pep2/elf18 and salt stress, respectively (Fig. 5C). Our analysis indicates a substantial overlap, but also a clear separation in the transcriptome between the biotic and abiotic stresses, in which a large portion of pattern-responsive genes is inherently not responsive to salt stress and *vice versa*.

Of 1,754 elf18- or Pep2-inducible DEGs and 2,611 salt-inducible DEGs, 281 genes (16.0%) and 222 genes (8.5%) were defined as PTST-DEGs,

respectively (Fig. 5C). Notably, these included pattern-specific DEGs which acquired salt inducibility following Pep1 pretreatment but were otherwise not responsive to salt stress: 3-d Pep1 pretreatment rendered 164 genes (125 + 39 genes in Supplementary Fig. S3A, relative to 1,285 genes, inherently salt-inducible) significantly induced at 3 h, and 24 genes (13 + 11 genes in Supplementary Fig. S3A, relative to 2,251 genes, inherently salt-inducible) at 24 h after salt stress. Moreover, PTST-DEGs included 264 genes, which were not among the elf18/Pep2-DEGs or salt-DEGs, but acquired salt inducibility in Pep1-pretreated plants (Fig. 5C). These results indicate that pre-activation of PRR signaling not only sensitizes salt stress responses but also broadens the range of target genes in salt stress responses, and emphasize that these effects are prominent early in salt responses.

We further dissected all the salt- and PTST-DEGs (Fig. 5B) by hierarchical clustering. The genes were classified into five clusters (Fig. 5D, Supplementary Table S1). GO analyses revealed no significant GO term enrichment for cluster 1, presumably due to the low number of genes (20 genes; Supplementary Table S1). Cluster 2, 3, 4 and 5 were overrepresented with lipid localization. Lipid is among the major components of the plasma membranes that are important not only for membrane remodeling i.e. adjusting membrane fluidity and permeability during salt stress, but also for numerous lipid signaling involved in the adaptation to salt and osmotic stress (Hou et al. 2016; Guo et al. 2019). Cluster 3 was also overrepresented with negative regulation of photosynthesis, consistent with the reduction of chlorophyll contents in the absence of Pep1-triggered salt tolerance (Fig. 1E, Fig. 3F). Cluster 4 was also overrepresented with negative regulation of root development, a hallmark response under salt stress (Acosta-Motos et al. 2017).

Notably, cluster 5 (2,194 genes) was over-represented with genes whose salt induction at 3 h was increased after Pep1 pretreatment (Fig 5D). It included a set of genes related to both defense and salt stress responses. For example, *PTR3*, encoding a putative peptide transporter, promotes both salt tolerance during seed germination and basal resistance to *Pst* DC3000 (Karim et al. 2007, 2005). *SnRK2.8* encodes an osmotic stress-activated protein kinase, which promotes drought tolerance (Umezawa et al. 2014) and systemic immunity by phosphorylating NPR1 (Lee et al. 2015). Interestingly, BON1 that negatively regulates cell death but positively regulates osmotic stress tolerance (Chen et al. 2020a) was found in this cluster. Thus, it seems likely that PRR signaling pre-activation leads to faster establishment of a salt stress-adapted transcriptome during PTST.

Transcriptional reprogramming during PTST

We then assembled salt-inducible genes that exhibited rapid induction following Pep1 pretreatment. Of the cluster 5 genes, 343 genes increased their salt induction at 3 h in Pep1-pretreated plants, while their induction was higher at 24 h than at 3 h in nontreated plants (Supplementary Fig. S3B). In their regulatory DNA sequences, within 1000-bp upstream of the transcriptional start sites, a motif enrichment analysis (CentriMo, Bailey & Machanick, 2012) revealed over-representation of the W box-containing sequences (58 out of 59 over-represented transcription factor binding sites, Supplementary Table S2). Four best-represented motifs were all prominent in the proximity to the transcription starting sites and included WRKY18- and WRKY40-specific DNA binding motifs (Fig. 5E, Supplementary Table S2), pointing to direct transcriptional regulation of these genes by WRKY18/WRKY40 during PTST.

WRKY18/WRKY40 negatively regulate flg22 induction of defense-related genes during PTI (Birkenbihl et al. 2017). Interestingly, WRKY18/WRKY40 target genes (Birkenbihl et al. 2017) were more clearly enriched in Cluster 5 genes displaying faster induction (149 out of 329 loci) compared to all Cluster 5 genes (471 out of 2083 loci) or PTST-DEGs (720 out of 5844 loci) (Fig. S3C), pointing to their role in rapid activation of a salt-induced transcriptome.

To test how WRKY18/WRKY40 are regulated during PTST, we conducted immunoblot analyses of functional HA-tagged WRKY18 and WRKY40 proteins expressed under the control of their native regulatory DNA sequences (*pWRKY18::WRKY18-HA wrky18* and *pWRKY40::WRKY40-HA wrky40*, respectively; Birkenbihl *et al*, 2017a). WRKY18 and WRKY40 accumulation was shown to be rapidly induced in response to flg22, with a peak of protein abundance at 1.5 h (Birkenbihl et al. 2017). WRKY18/WRKY40 accumulation was reduced to nearly background levels 4 d after Pep1 application (0 h NaCl, Fig. 5F). WRKY40-HA accumulation became strongly induced 1 h after salt stress, and then diminished (Fig. 5F), indicating that there is transient WRKY40 induction during PTI and salt stress. Importantly, Pep1 pretreatment markedly elevated and prolonged salt-induced WRKY40-HA accumulation up to 24 h (Fig. 5F), following its increased mRNA expression (Fig. S3D). A similar Pep1 effect was observed for WRKY18-HA accumulation (Fig. 5F). These results suggest that PRR signaling pre-activation leads to enhanced and durable accumulation of both WRKY40 and WRKY18 under salt stress.

In contrast to Cluster 5, Cluster 4 was characterized by salt-inducible genes at 24 h, whose induction was suppressed after Pep1 pretreatment (Fig. S4). Without PTST, their induction was prominent at 24 h compared to 3h, and may rather reflect salt stress symptom than salt stress tolerance. A motif enrichment

analysis in their regulatory DNA sequences as described above revealed over-representation of three transcription factor binding motifs, namely WRKY31, ANAC047 and WRKY20 (Fig. S4, Supplementary Table S1), implying that Pep1 sensitization and Pep1 desensitization of salt-inducible genes occur through distinct sets of transcription factors. Although *ANAC047* has been implicated in waterlogging responses and leaf senescence (Rauf et al., Plant Cell 2013), the other two have been poorly characterized to date.

Non-pathogenic bacteria confer PTST

Since bacterial MAMP application confers salt tolerance (Fig. 3), we tested whether immune recognition of bacteria also leads to salt tolerance. To this end, we determined the effects of pre-inoculation with different strains of *Pst* DC3000 on salt stress tolerance: *Pst* DC3000 *ΔhrpS*, impaired in the expression of the type III effectors (Hutcheson et al. 2001) and conventionally used as a PTI trigger, and *Pst* DC3000 *AvrRpm1* or *Pst* DC3000 *AvrRps4*, inducing ETI conferred by the CC-NLR RPM1 and the TIR-NLR pair RRS1-S/RPS4, respectively (Grant et al. 1995; Gassmann et al. 1999; Saucet et al. 2015). All of these bacterial strains fail to grow in the WT plants used here, which harbor the cognate NLRs. Pre-inoculation with *Pst* DC3000 *ΔhrpS* significantly enhanced the survival rate of seedlings under salt stress, whereas *Pst* DC3000 *AvrRpm1* or *Pst* DC3000 *AvrRps4* did not (Fig. 6A). Without salt stress, plant survival rates were essentially indistinguishable between these non-pathogenic and avirulent strains (Supplementary Table S2). These results suggest that PRR recognition, but not NLR recognition of live bacteria, effectively confers salt tolerance.

Notably, bacterium-triggered salt tolerance was strongly reduced in the PRR mutants and PRR-associated kinase mutants, *fls2 efr* and *bak1-5 bkk1-1*, respectively (Fig. 6B-C), as in MAMP/DAMP-triggered salt tolerance (Fig. 1-3). Basal salt tolerance under sterile conditions (in mock controls without bacteria) was significantly lowered in *bak1 bkk1* plants but was unaffected in *fls2 efr* plants (Fig. 6B-C), pointing to involvement of a BAK1-dependent DAMP receptor(s) but not MAMP receptors FLS2/EFR in basal salt tolerance. Pre-inoculation with nonpathogenic PTI-triggering bacterium, *Pseudomonas simiae* WCS417 (*Pfo* abbreviated after *Pseudomonas fluorescence*) also conferred salt tolerance, which was abolished in *bak1-5 bkk1* plants (Fig. 6D). The results suggest that the PRR signaling module becomes engaged in response to bacterial challenge, thereby conferring salt tolerance.

Finally, we tested whether bacterial MAMP recognition without live bacteria is sufficient to acquire salt tolerance. Indeed, pre-inoculation with heat-killed *Pfo* enhanced salt tolerance in a *BAK1/BKK1*-dependent manner (Fig. 6E). Collectively, these results suggest that PRRs are important for salt stress sensing and adaptation when recognizing molecular patterns derived from the host-associated microbes or cellular damage.

DISCUSSION

Immune receptor activation can positively or negatively influence abiotic stress responses, yet the molecular logic behind this signaling plasticity remains poorly understood. Here, we show that PRR signaling triggers an enhanced or primed state of salt stress tolerance in plants (Fig. 1, Fig. 3, Table 1). Several lines of evidence indicate that PTST and PTI share previously described key steps within and proximal to the receptor complexes, at least for three *BAK1*-

dependent PRR pathways. A failure to mount PTST in the *bak1-5* mutant and in the absence of *BIK1/PBL1* or *RBOHD* indicates that PTST is achieved by authentic PRR signaling (Fig. 2, Fig. 3, Fig. 6). Effective cross-tolerance to biotic and salt stresses following PRR signaling may reflect similar cellular states and requirements in these stress conditions. This notion is supported by a substantial overlap between the pattern-induced and salt-induced transcriptomes (Fig. 5, Supplementary Fig. S1). Recent study also reported that rapidly induced genes in response to different MAMPs/DAMPs tend to be also induced under various abiotic stresses (Bjornson et al, 2021). Consistently, pattern recognition leads to the sensitization of salt-responsive genes and mobilization of otherwise non-responsive genes, most prominently during early responses to salt stress (Fig. 5, Supplementary Fig. S1 and S3). These findings indicate rapid activation and expansion of the salt-responsive transcriptome as an important basis for PTST. By focusing on genes whose salt induction is strengthened and/or accelerated following Pep1 application, we revealed an interesting set of PTST-characteristic DEGs (Fig. 5D, Supplementary Table S1).

DAMPs represent a common signature of biotic and abiotic stress conditions in animals and plants (Gust et al. 2017; De Lorenzo et al. 2018). In plants, abiotic modulation of cell walls and phospholipid membranes generates a battery of DAMPs (Chen et al. 2020b; Rui and Dinneny 2020; Herger et al. 2019; Jiang et al. 2019). Although the identity of cognate DAMP ligands remains elusive, different RKs are involved in mediating PTI-like defense responses and salt tolerance under salt stress conditions (Feng et al. 2018; Engelsdorf et al. 2018; van der Does et al. 2017). Here, we show that PROPEP3, together with short fragments likely containing its C-terminal Pep3 epitope, is released following salt stress, without microbes or exogenous

MAMP/DAMP application (Fig. 4A-B). *PROPEP2/PROPEP3* expression represents an important preparatory step for positive feedback of defense signaling through PEPRs (Ross *et al*, 2014). *PROPRP2/PROPEP3* were among the 343 genes displaying faster salt induction following PRR activation (Supplementary Fig. S3C), pointing to a role for the PEPR pathway in rapid mobilization of salt-adaptive responses during PTST. Indeed, *PEPRs* provide a rate-limiting step in salt tolerance and salt-induced osmotic stress tolerance, both under sterile conditions (Fig. 4C-D). Genetic requirements for *BAK1* and *BIK1/PBL1* (Fig. 2, Fig. 3, Fig. 6C-E) are consistent with the involvement of *BAK1/BIK1*-dependent DAMP receptors, including PEPRs, in salt tolerance. These findings strengthen the view that PRRs contribute to salt tolerance.

Shared use of common signaling components between PTI and salt tolerance extends beyond *BAK1/BIK1*-dependent PRR pathways. Glycosyl inositol phosphorylceramide sphingolipids provide Na^+ sensors to induce Ca^{2+} influx for SOS signaling under salt stress (Jiang et al. 2019), and also perception sites for bacterial/fungal/oomycete Necrosis and ethylene-inducing peptide 1-like (NLP) proteins (Lenarčič et al. 2017). Salt tolerance is dependent on the *Catharanthus roseus* RK *FER* (Feng et al. 2018; Zhao et al. 2018). FER recognizes immunostimulatory and immunosuppressive members of the endogenous RALF peptides and also scaffolds different PRR complexes (Stegmann et al. 2017; Haruta et al. 2014). FER-mediated salt tolerance in part depends on its ability to bind pectin and protect pectin crosslinking, suggesting its role in the sensing and management of cell wall integrity under salt stress (Feng et al. 2018). Following S1P subtilase cleavage, RALF22/RALF23 are released from LRR-containing extensins LRX3/LRX4/LRX5, thereby lowering salt tolerance through FER (Zhao et al. 2018). Notably, S1P-cleaved RALF

members attenuate both FER-mediated salt tolerance and PTI (Zhao et al. 2018; Stegmann et al. 2017). These studies further highlight the resemblance of PTI and salt stress signaling. Under our conditions, however, chitin signaling pre-activation failed to confer salt tolerance. The apparent discrepancy between our and previous studies of chitin/CERK1-mediated salt tolerance (Supplementary Fig. S1) (Brotman *et al*, 2012; Espinoza *et al*, 2017) might reflect a divergence between different ectodomain classes of PRRs in their optimal conditions for salt tolerance, as seen in their regulation of immunity (Saijo et al. 2018).

Successful induction of PTST by PRR recognition of bacterial MAMPs, but not by NLR recognition of their effectors (Fig. 3, Fig. 6), fits with the idea that strong activation of immunity negatively influences salt tolerance. This is in line with previously studies that *EDS1/PAD4*-mediated defense activation results in the collapse of osmotic stress tolerance (Ariga et al. 2017). This cross-tolerance trade-off predicts the existence of a critical threshold beyond which further immune activation comes at a cost for salt and osmotic stress tolerance. Recent studies show that PRR signaling provides an integrating basis for ETI, and that mutual PTI-ETI potentiation is required for effective pathogen resistance (Ngou et al. 2021; Yuan et al. 2021). At present, how NLR signaling exceeds the predicted threshold during ETI remains poorly understood.

Mostly from soil microbes, plants selectively recruit and modify their root-associated microbiota during adaptation to different stress conditions (Shilev 2020). It is conceivable that these changes under salt stress are accompanied by alterations in the presentation of MAMPs/DAMPs in the extracellular milieu, as shown for PROPEP3 (Fig. 4B), which are sensed and linked by PRRs to adaptive responses to salt stress. It has been described that non-pathogenic

556 microbes serve to alleviate salt stress in the host plant (Egamberdieva et al.
557 2019; Fan et al. 2020; Zuccaro et al. 2011). In addition to the beneficial
558 activities of specific plant-associated bacteria, our work indicates that PRR
559 recognition of bacterial MAMPs, not their live activities, leads to plant salt
560 tolerance. This study unravels a fraction of plant-microbe-environment
561 interactions, in which endogenous or microbial immunogenic patterns
562 generated under salt stress likely engage PRRs in promoting salt/osmotic
563 stress tolerance, in part by priming the activation of salt-adaptive transcriptome
564 (Fig. 7).
565
566

567 **MATERIALS AND METHODS**

568 **Plant materials and growth conditions**

569 The *A. thaliana* accession Col-0 was used as WT. Plant materials used are
570 provided in Supplementary Table S4. Seeds were sterilized with 6% sodium
571 hypochlorite and 0.1% Triton X-100 for 15 minutes, rinsed 5 times with
572 autoclaved distilled water and stratified at 4 ℃ for 2-5 days before use. The
573 growth medium used was Murashige and Skoog (MS) medium (1/2 strength MS
574 basal salts, 25 mM sucrose, 0.5 g/L MES, pH 5.7) unless otherwise stated.
575 Plants were grown under 14 h light/ 10 h dark at 22 ℃ unless otherwise stated.
576 For detection of extracellular PROPEP3-Venus protein, two-week-old seedlings
577 in liquid growth media were exposed to 0.5 μM Pep1 for 3 days, 150 mM NaCl
578 for 3 days or 0.5 μM Pep1 for 12 h followed by 150 mM NaCl for 3 days under
579 standard growth conditions.
580

581 **Pattern-triggered salt tolerance assay**

Four-day-old seedlings in the liquid growth media were treated with the indicated elicitors (0.1 μM Peps/flg22/elf18, 100 μg/ml chitin). For treatment with heat-killed bacteria, bacteria cultivated (as described below) up to OD_{590} = 0.2 were collected, suspended and then autoclaved at 121°C for 20 minutes. The supernatants after centrifugation were recovered for use. Four days after elicitor/bacterium treatments, seedlings were transferred to the agar growth media supplemented with 150 or 175 mM NaCl. The number of viable seedlings was scored every day for the indicated duration. Survival ratio was determined as the number of viable seedlings relative to the total number of seedlings used. For fresh weight determination, seedlings were pooled for weighing and the average weight per seedling was determined by dividing the weight by the number of seedlings pooled. Chlorophyll contents were determined essentially as described previously (Porra et al. 1989 Biochimica et Biophysica Acta), except the chlorophyll contents were normalized by the number of seedlings used.

Acquired osmotic tolerance assay

Assays for salt-induced osmotic stress tolerance were performed as described in Ariga *et al*, 2017. In brief, 7-d-old seedlings were transferred from agar growth media to that supplemented with 100 mM NaCl, and further incubated for 7 days. Seedlings were then transferred to that supplemented with 750 mM sorbitol, and grown for another 14 days before the determination of chlorophyll contents.

Quantitative RT-PCR analysis

Total RNA was extracted from plant samples with Purelink (Nacalai Tesque,

Japan) and reverse transcribed with PrimeScript Reagent Kit Perfect Real Time (Takara, Japan) according to manufacturer's instructions. qRT-PCR was performed with Power SYBR Green PCR Master Mix (Applied Biosystems, Japan) using the Thermal Cycler Dice RealTime TP870 (Takara, Japan) under the following conditions: 50°C 2 min, 95°C 10 min, 95°C 15 s followed by 60°C 1 min for 40 cycles, then 95°C 15 s, 60°C 30 s, and finally 95°C 15 s. The primers used are provided in Appendix Table 4.

Protein extraction and immunoblot analysis

Protein extracts were prepared by homogenizing frozen tissues in a lysis buffer [50 mM Tris- HCl pH7.5, 2% SDS, 2mM DTT, 2.5 mM NaF, P9599 protease inhibitor cocktail (Sigma)] for 15 min at room temperature. The supernatants recovered after centrifugation at 13,000 g for 15 minutes were subjected to immunoblot analysis on 10% SDS-PAGE with the indicated antibodies, enlisted below. Molecular weight markers used was Protein Ladder One (Triple- color; Nacalai Tesque, Japan). Anti-HA (3F10) antibody was purchased from Roche. Anti-PROPEP3 antibodies raised in rabbits against both N- and C-terminal fragments of PROPEP3 were described previously (Ross et al., 2014). For detection of extracellular PROPEP3-Venus pool, protein concentrated from the liquid media with Strataclean resin (Agilent Technologies) after filtration was used as an extracellular fraction.

RNA sequencing and analysis

Five-day-old seedlings grown as described above were pretreated with 0.1 μM Pep1 for 3 days and then exposed to 150 mM NaCl for the indicated times. Three biological replicates were prepared per treatment and genotype. Total

RNA was extracted with an RNA extraction kit following the manufacturer's procedures (NucleoSpin RNA, Machery-Nagel). Each cDNA library was prepared using a TruSeq RNA Library Prep Kit v2 following the manufacturer's procedures (Illumina, USA). High-throughput sequencing was run by single read 50-bp on a HiSeq2500 platform (Illumina). Raw sequence data were deposited in the DDBJ Sequence Read Archive (accession number DRA004299). Reads were mapped to the TAIR9 Arabidopsis transcriptome database (https://www.arabidopsis.org). The edgeR software package (bioconductor.org.packages/release/bioc/html/edgeR.html) was used for estimation of false discovery rate (FDR) for differential gene expression of raw reads from all 3 biological replicates.

All mRNA variants detected from a gene locus were defined as separate genes in RNA-seq analyses, but assembled and scored for the one gene locus in cross-referencing RNA-seq and ChIP-seq data. For instance, 343 genes were scored as DEGs displaying faster salt induction after Pep1 pretreatment in our RNA-seq analysis, while they were scored as 329 genes corresponding to their loci in the cross-referenced ChIP-seq data. Heatmap was generated with an R-software heat map tool from gplot package (https://cran.r-project.org/web/packages/gplots/) with differentially expressed genes (DEGs) identified using the following cut-off values: FDR <0.05, expression $|\log_2 FC \geq 1]$ and Student's t-test p <0.05. Gene read counts were normalized to RPKM values, and hierarchical clustering was conducted with one minus Pearson correlation complete linkage.

Bacterial inoculation for salt tolerance assay

660 *Pseudomonas syringae* DC3000 ⊿ *hrpS* (Jovanovic et al. 2011), *AvrRpm1*
661 (Debener et al. 1991), *AvrRps4* (Sohn et al. 2009) and *Pseudomonas simiae*
662 WCS417 (Berendsen et al. 2015) were grown in NYGB media (5 g/L peptone, 3
663 g/L yeast extract, 20 mL/L glycerol, pH7.0) supplemented with appropriate
664 antibiotics (rifampicin 25 mg/mL in DMSO, kanamycin 50 mg/mL in deionized
665 distilled water (ddH_2O), tetracycline 15 mg/L in ethanol, chloramphenicol 30
666 mg/mL in ethanol). Overnight bacterial cultures were washed at least twice with
667 10 mM $MgCl_2$ and then adjusted to OD_{590} = 0.002 for spray inoculation.
668 Seedlings were transferred from liquid growth media to agar plates 1 day prior
669 to spray-inoculation. At 6 h after inoculation, seedlings were surface-sterilized
670 twice with 70% ethanol, rinsed twice with autoclaved H_2O and then transferred
671 to agar media supplemented with or without 175 mM NaCl.

673 **Acknowledgments**

674 We thank the Saijo Lab members for technical assistance and insightful
675 discussions, and Drs. Yasunari Fujita, Fumiaki Katagiri, Jian-Min Zhou and Cyril
676 Zipfel for published materials. The RNA sequencing was supported by the
677 Cooperative Research Program of the Genome Research for BioResource,
678 NODAI Genome Research Center, Tokyo University of Agriculture.

679

680 **Author contributions**

681 YS conceived the study. EL, KY and YS designed the experiments. EL, YT, KY,
682 TH, HA and TF developed and performed the experiments. EL, YT, KY, HA, KT
683 and TT analyzed the data. IS and JP provided materials and advised on the
684 experiments. EL and YS wrote the manuscript with contributions from the other
685 authors.

686

687 **Conflict of interest**

688 The authors declare that they have no conflict of interest.

689

690 **REFERENCES**

691

692 Acosta-Motos, J. R., Ortuño, M. F., Bernal-Vicente, A., Diaz-Vivancos, P.,
693 Sanchez-Blanco, M. J., and Hernandez, J. A. 2017. Plant Responses to
694 Salt Stress: Adaptive Mechanisms. Agronomy. 7
695 Ariga, H., Katori, T., Tsuchimatsu, T., Hirase, T., Tajima, Y., Parker, J., Alcázar,
696 R., Koornneef, M., Hoekenga, O., Lipka, A., Gore, M., Sakakibara, H.,
697 Kojima, M., Kobayashi, Y., Iuchi, S., Kobayashi, M., Shinozaki, K., Sakata,
698 Y., Hayashi, T., Saijo, Y., and Taji, T. 2017. NLR locus-mediated trade-off
699 between abiotic and biotic stress adaptation in Arabidopsis. Nat. Plants.
700 3:17072
701 Aslam, S., Erbs, G., Morrissey, K., Newman, M., Chinchilla, D., Boller, T.,
702 Molinaro, A., Jackson, R., and Cooper, R. 2009. Microbe-associated
703 molecular pattern (MAMP) signatures, synergy, size and charge: influences
704 on perception or mobility and host defence responses. Mol. Plant Pathol.
705 10:375–87
706 Bailey, T., and Machanick, P. 2012. Inferring direct DNA binding from ChIP-seq.
707 Nucleic Acids Res. 40:e128
708 Bartels, S., Lori, M., Mbengue, M., van Verk, M., Klauser, D., Hander, T., Böni,
709 R., Robatzek, S., and Boller, T. 2013. The family of Peps and their
710 precursors in Arabidopsis: differential expression and localization but
711 similar induction of pattern-triggered immune responses. J. Exp. Bot.
712 64:5309–21
713 Bartsch, M., Gobbato, E., Bednarek, P., Debey, S., Schultze, J., Bautor, J., and
714 Parker, J. 2006. Salicylic acid-independent ENHANCED DISEASE
715 SUSCEPTIBILITY1 signaling in *Arabidopsis* immunity and cell death is

716 regulated by the monooxygenase *FMO1* and the Nudix hydrolase *NUDT7*.
717 Plant Cell. 18:1038–51
718 Berendsen, R., van Verk, M., Stringlis, I., Zamioudis, C., Tommassen, J.,
719 Pieterse, C., and Bakker, P. 2015. Unearthing the genomes of plant-
720 beneficial Pseudomonas model strains WCS358, WCS374 and WCS417.
721 BMC Genomics. 16:539
722 Birkenbihl, R., Kracher, B., Roccaro, M., and Somssich, I. 2017. Induced
723 Genome-Wide Binding of Three Arabidopsis WRKY Transcription Factors
724 during Early MAMP-Triggered Immunity. Plant Cell. 29:20–38
725 Boller, T., and Felix, G. 2009. A Renaissance of Elicitors: Perception of
726 Microbe-Associated Molecular Patterns and Danger Signals by Pattern-
727 Recognition Receptors. Annu. Rev. Plant Biol. 60:379–406
728 Brotman, Y., Landau, U., Pnini, S., Lisec, J., Balazadeh, S., Mueller-Roeber, B.,
729 Zilberstein, A., Willmitzer, L., Chet, I., and Viterbo, A. 2012. The LysM
730 receptor-like kinase LysM RLK1 is required to activate defense and abiotic-
731 stress responses induced by overexpression of fungal chitinases in
732 *Arabidopsis* plants. Mol. Plant. 5:1113–24
733 Chen, K., Gao, J., Sun, S., Zhang, Z., Yu, B., Li, J., Xie, C., Li, G., Wang, P.,
734 Song, C.-P., Bressan, R. A., Hua, J., Zhu, J.-K., and Yang, Z. 2020a.
735 BONZAI Proteins Control Global Osmotic Stress Responses in Plants.
736 Curr. Biol. 30:4815-4825.E4
737 Chen, Y., Fan, K., Hung, S., and Chen, Y. 2020b. The role of peptides cleaved
738 from protein precursors in eliciting plant stress reactions. New Phytol.
739 225:2267–82
740 Couto, D., and Zipfel, C. 2016. Regulation of pattern recognition receptor
741 signalling in plants. Nat. Rev. Immunol. 16:537–52

Cui, H., Gobbato, E., Kracher, B., Qiu, J., Bautor, J., and Parker, J. 2017. A core function of EDS1 with PAD4 is to protect the salicylic acid defense sector in Arabidopsis immunity. New Phytol. 213:1802–17

Cui, H., Tsuda, K., and Parker, J. 2015. Effector-triggered immunity: from pathogen perception to robust defense. Annu. Rev. Plant Biol. 66:487–511

Cutler, S., Rodriguez, P., Finkelstein, R., and Abrams, S. 2010. Abscisic acid: emergence of a core signaling network. Annu. Rev. Plant Biol. 61:651–79

Debener, T., Lehnackers, H., Arnold, M., and Dangl, J. 1991. Identification and molecular mapping of a single *Arabidopsis thaliana* locus determining resistance to a phytopathogenic *Pseudomonas syringae* isolate. Plant J. 1:289–302

DeFalco, T., and Zipfel, C. 2021. Molecular mechanisms of early plant pattern-triggered immune signaling. Mol. Cells. 81:3449–67

Ding, P., and Ding, Y. 2020. Stories of Salicylic Acid: A Plant Defense Hormone. Trends Plant Sci. :DOI: 10.1016/j.tplants.2020.01.004

van der Does, D., Boutrot, F., Engelsdorf, T., Rhodes, J., McKenna, J., Vernhettes, S., Koevoets, I., Tintor, N., Veerabagu, M., Miedes, E., Segonzac, C., Roux, M., Breda, A., Hardtke, C., Molina, A., Rep, M., Testerink, C., Mouille, G., Höfte, H., Hamann, T., and Zipfel, C. 2017. The Arabidopsis leucine-rich repeat receptor kinase MIK2/LRR-KISS connects cell wall integrity sensing, root growth and response to abiotic and biotic stresses. PLOS Genet. 13:e1006832

Dongus, J. A., and Parker, J. E. 2021. EDS1 signalling: At the nexus of intracellular and surface receptor immunity. Curr. Biol. 62:102039

Egamberdieva, D., Wirth, S., Bellingrath-Kimura, Sonoko Dorothea Mishra, J., and Arora, N. K. 2019. Salt-Tolerant Plant Growth Promoting Rhizobacteria

for Enhancing Crop Productivity of Saline Soils. Front. Microbiol. 10:2791

Engelsdorf, T., Gigli-Bisceglia, N., Veerabagu, M., McKenna, J., Vaahtera, L., Augstein, F., van der Does, D., Zipfel, C., and Hamann, T. 2018. The plant cell wall integrity maintenance and immune signaling systems cooperate to control stress responses in *Arabidopsis thaliana*. Sci. Signal. 11:eaao3070

Espinoza, C., Liang, Y., and Stacey, G. 2017. Chitin receptor CERK1 links salt stress and chitin-triggered innate immunity in Arabidopsis. Plant J. 89:984–95

Fan, D., Subramanian, S., and Smith, D. L. 2020. Plant endophytes promote growth and alleviate salt stress in *Arabidopsis thaliana*. Sci. Rep. 10:12740

Feng, W., Kita, D., Peaucelle, A., Cartwright, H., Doan, V., Duan, Q., Liu, M., Maman, J., Steinhorst, L., Schmitz-Thom, I., Yvon, R., Kudla, J., Wu, H., Cheung, A., and Dinneny, J. 2018. The FERONIA Receptor Kinase Maintains Cell-Wall Integrity during Salt Stress through Ca^{2+} Signaling. Curr. Biol. 28:666–75.e5

Finkelstein, R. 2013. Abscisic Acid synthesis and response. Arab. B. 11:e0166

Gassmann, W., Hinsch, M., and Staskawicz, B. 1999. The Arabidopsis RPS4 bacterial-resistance gene is a member of the TIR-NBS-LRR family of disease-resistance genes. Plant J. 20:265–77

Geng, Y., Wu, R., Wee, C., Xie, F., Wei, X., Chan, P., Tham, C., Duan, L., and Dinneny, J. 2013. A spatio-temporal understanding of growth regulation during the salt stress response in *Arabidopsis*. Plant Cell. 25:2132–54

Glazebeook, J., Chen, W., Estes, B., Chang, H., Nawrath, C., Métraux, J., Zhu, T., and Katagiri, F. 2003. Topology of the network integrating salicylate and jasmonate signal transduction derived from global expression phenotyping. Plant J. 34:217–28

794 Gómez-Gómez, L., and Boller, T. 2000. FLS2: an LRR receptor-like kinase
795 involved in the perception of the bacterial elicitor flagellin in *Arabidopsis*.
796 Mol. CellsCell. 5:1003–11
797 Gómez-Gómez, L., Felix, G., and Boller, T. 1999. A single locus determines
798 sensitivity to bacterial flagellin in *Arabidopsis thaliana*. Plant J. 18:277–84
799 González-Guzmán, M., Apostolova, N., Bellés, J., Barrero, J., Piqueras, P.,
800 Ponce, M., Micol, J., Serrano, R., and Rodríguez, P. 2002. The short-chain
801 alcohol dehydrogenase ABA2 catalyzes the conversion of xanthoxin to
802 abscisic aldehyde. Plant Cell. 14:1833–46
803 Grant, M., Godiard, L., Straube, E., Ashfield, T., Lewald, J., Sattler, A., Innes,
804 R., and Dangl, J. 1995. Structure of the Arabidopsis RPM1 gene enabling
805 dual specificity disease resistance. Science. 269:843–6
806 Guo, Q., Liu, L., and Barkla, B. J. 2019. Membrane Lipid Remodeling in
807 Response to Salinity. Int. J. Mol. Sci. 20:4264
808 Gust, A., Pruitt, R., and Nürnberger, T. 2017. Sensing Danger: Key to Activating
809 Plant Immunity. Trends Plant Sci. 22:779–91
810 Hander, T., Fernández-Fernández, Á., Kumpf, R., Willems, P., Schatowitz, H.,
811 Rombaut, D., Staes, A., Nolf, J., Pottie, R., Yao, P., Gonçalves, A., Pavie,
812 B., Boller, T., Gevaert, K., Van Breusegem, F., Bartels, S., and Stael, S.
813 2019. Damage on plants activates Ca^{2+}-dependent metacaspases for
814 release of immunomodulatory peptides. Science. 363:eaar7486
815 Haruta, M., Sabat, G., Stecker, K., Minkoff, B., and Sussman, M. 2014. A
816 peptide hormone and its receptor protein kinase regulate plant cell
817 expansion. Science. 343:408–11
818 Herger, A., Dünser, K., Kleine-Vehn, J., and Ringli, C. 2019. Leucine-Rich
819 Repeat Extensin Proteins and Their Role in Cell Wall Sensing. Curr. Biol.

29:R851–R858

Hou, Q., Ufer, G., and Bartels, D. 2016. Lipid signalling in plant responses to abiotic stress. Plant Cell Environ. 39:1029–48

Hutcheson, S., Bretz, J., Sussan, T., Jin, S., and Pak, K. 2001. Enhancer-binding proteins HrpR and HrpS interact to regulate hrp-encoded type III protein secretion in *Pseudomonas syringae* strains. J. Bacteriol. 183:5589–98

Jiang, Z., Zhou, X., Tao, M., Yuan, F., Liu, L., Wu, F., Wu, X., Xiang, Y., Niu, Y., Liu, F., Li, C., Ye, R., Byeon, B., Xue, Y., Zhao, H., Wang, H., Crawford, B., Johnson, D., Hu, C., Pei, C., Zhou, W., Swift, G., Zhang, H., Vo-Dinh, T., Hu, Z., Siedow, J., and Pei, Z. 2019. Plant cell-surface GIPC sphingolipids sense salt to trigger Ca^{2+} influx. Nature. 572:341–46

Jones, J., and Dangl, J. 2006. The plant immune system. Nature. 444:323–9

Jones, J., Vance, R., and Dangl, J. 2016. Intracellular innate immune surveillance devices in plants and animals. Science. 354:aaf6395

Jovanovic, M., James, E., Burrows, P., Rego, F., Buck, M., and Schumacherb, J. 2011. Regulation of the co-evolved HrpR and HrpS AAA+ proteins required for *Pseudomonas syringae* pathogenicity. Nat. Commun. 2:177

Kadota, Y., Shirasu, K., and Zipfel, C. 2015. Regulation of the NADPH Oxidase RBOHD during Plant Immunity. Plant Cell Physiol. 56:1472–80

Karim, S., Holmström, K., Mandal, A., Dahl, P., Hohmann, S., Brader, G., Palva, E., and Pirhonen, M. 2007. *At*PTR3, a wound-induced peptide transporter needed for defence against virulent bacterial pathogens in Arabidopsis. Planta. 225:1431–45

Karim, S., Lundh, D., Holmström, K., Mandal, A., and Pirhonen, M. 2005. Structural and functional characterization of *At*PTR3, a stress-induced

846 peptide transporter of Arabidopsis. J. Mol. Model. 11:226–36

847 Kim, M., da Cunha, L., McFall, A., Belkhadir, Y., DebRoy, S., Dangl, J., and
848 Mackey, D. 2005. Two *Pseudomonas syringae* type III effectors inhibit
849 RIN4-regulated basal defense in *Arabidopsis*. Cell. 121:749–59

850 Krol, E., Mentzel, T., Chinchilla, D., Boller, T., Felix, G., Kemmerling, B., Postel,
851 S., Arents, M., Jeworutzki, E., Al-Rasheid, K., Becker, D., and Hedrich, R.
852 2010. Perception of the *Arabidopsis* danger signal peptide 1 involves the
853 pattern recognition receptor *At*PEPR1 and its close homologue *At*PEPR2.
854 J. Biol. Chem. 285:13471–9

855 Lee, H., Park, Y., Seo, P., Kim, J., Sim, H., Kim, S., and Park, C. 2015.
856 Systemic Immunity Requires SnRK2.8-Mediated Nuclear Import of NPR1 in
857 Arabidopsis. Plant Cell. 27:3425–38

858 Lenarčič, T., Albert, I., Böhm, H., Hodnik, V., Pirc, K., Zavec, A., Podobnik, M.,
859 Pahovnik, D., Žagar, E., Pruitt, R., Greimel, P., Yamaji-Hasegawa, A.,
860 Kobayashi, T., Zienkiewicz, A., Gömann, J., Mortimer, J., Fang, L.,
861 Mamode-Cassim, A., Deleu, M., Lins, L., Oecking, C., Feussner, I.,
862 Mongrand, S., Anderluh, G., and Nürnberger, T. 2017. Eudicot plant-
863 specific sphingolipids determine host selectivity of microbial NLP
864 cytolysins. Science. 358:1431–4

865 De Lorenzo, G., Ferrari, S., Cervone, F., and Okun, E. 2018. Extracellular
866 DAMPs in Plants and Mammals: Immunity, Tissue Damage and Repair.
867 Trends Immunol. 39:937–50

868 Nakaminami, K., Okamoto, M., Higuchi-Takeuchi, M., Yoshizumi, T.,
869 Yamaguchi, Y., Fukao, Y., Shimizu, M., Ohashi, C., Tanaka, M., Matsui,
870 M., Shinozaki, K., Seki, M., and Hanada, K. 2018. *At*Pep3 is a hormone-
871 like peptide that plays a role in the salinity stress tolerance of plants. Proc.

Natl. Acad. Sci. 115:5810–15

Ngou, B., Ahn, H.-K., Ding, P., and Jones JDG. 2021. Mutual Potentiation of Plant Immunity by Cell-surface and Intracellular Receptors. Nature. 592:110–5

Pieterse, C., van der Does, D., Zamioudis, C., Leon-Reyes, A., and Van Wees, S. 2012. Hormonal modulation of plant immunity. Annu. Rev. Cell Dev. Biol. 28:489–521

Ross, A., Yamada, K., Hiruma, K., Yamashita-Yamada, M., Lu, X., Takano, Y., Tsuda, K., and Saijo, Y. 2014. The Arabidopsis PEPR pathway couples local and systemic plant immunity. EMBO J. 33:62–75

Roux, M., Schwessinger, B., Albrecht, C., Chinchilla, D., Jones, A., Holton, N., Malinovsky, F. G., Tör, M., de Vries, S., and Zipfel, C. 2011. The *Arabidopsis* Leucine-Rich Repeat Receptor–Like Kinases BAK1/SERK3 and BKK1/SERK4 Are Required for Innate Immunity to Hemibiotrophic and Biotrophic Pathogens. Plant Cell. 23:2440–55

Rui, Y., and Dinneny, J. 2020. A wall with integrity: surveillance and maintenance of the plant cell wall under stress. New Phytol. 225:1428–39

Saijo, Y., and Loo, E. 2020. Plant immunity in signal integration between biotic and abiotic stress responses. New Phytol. 225:87–104

Saijo, Y., Loo, E., and Yasuda, S. 2018. Pattern recognition receptors and signaling in plant-microbe interactions. Plant J. 93:591–613

Saucet, S., Ma, Y., Sarris, P., Furzer, O., Sohn, K., and Jones JDG. 2015. Two linked pairs of Arabidopsis TNL resistance genes independently confer recognition of bacterial effector AvrRps4. Nat. Commun. 6:6338

Schwessinger, B., Roux, M., Kadota, Y., Ntoukakis, V., Sklenar, J., Jones, A., and Zipfel, C. 2011. Phosphorylation-dependent differential regulation of

plant growth, cell death, and innate immunity by the regulatory receptor-like kinase BAK1. PLoS Genet. 7:e1002046

Shilev, S. 2020. Plant-Growth-Promoting Bacteria Mitigating Soil Salinity Stress in Plants. Appl. Sci. 10:7326

Sohn, K., Zhang, Y., and Jones, J. 2009. The *Pseudomonas syringae* effector protein, AvrRPS4, requires in planta processing and the KRVY domain to function. Plant J. 57:1079–91

Stegmann, M., Monaghan, J., Smakowska-Luzan, E., Rovenich, H., Lehner, A., Holton, N., Belkhadir, Y., and Zipfel, C. 2017. The receptor kinase FER is a RALF-regulated scaffold controlling plant immune signaling. Science. 355:287–9

Tsuda, K., Sato, M., Stoddard, T., Glazebrook, J., and Katagiri, F. 2009. Network properties of robust immunity in plants. PLoS Genet. 12:e1000772

Umezawa, T., Yoshida, R., Maruyama, K., Yamaguchi-Shinozaki, K., and Shinozaki, K. 2014. SRK2C, a SNF1-related protein kinase 2, improves drought tolerance by controlling stress-responsive gene expression in *Arabidopsis thaliana*. Proc. Natl. Acad. Sci. 101:17306–11

Velásquez, A., Castroverde, C., and He, S. 2018. Plant-Pathogen Warfare under Changing Climate Conditions. Curr. Biol. 28:R619–R634

Vlot, A., Dempsey, D., and Klessig, D. 2009. Salicylic Acid, a multifaceted hormone to combat disease. Annu. Rev. Phytopathol. 47:177–206

Wiermer, M., Feys, B., and Parker, J. 2005. Plant immunity: the EDS1 regulatory node. Curr. Opin. Plant Biol. 8:383–9

Wildermuth, M., Dewdney, J., Wu, G., and Ausubel, F. 2001. Isochorismate synthase is required to synthesize salicylic acid for plant defence. Nature. 414:562–5

924 Yamada, K., Yamashita-Yamada, M., Hirase, T., Fujiwara, T., Tsuda, K.,
925 Hiruma, K., and Saijo, Y. 2016. Danger peptide receptor signaling in plants
926 ensures basal immunity upon pathogen-induced depletion of BAK1. EMBO
927 J. 35:46–61
928 Yamaguchi, Y., Huffaker, A., Bryan, A., Tax, F., and Ryan, C. 2010. PEPR2 is a
929 second receptor for the Pep1 and Pep2 peptides and contributes to
930 defense responses in Arabidopsis. Plant Cell. 22:508–22
931 Yamaguchi, Y., Pearce, G., and Ryan, C. A. 2006. The cell surface leucine-rich
932 repeat receptor for AtPep1, an endogenous peptide elicitor in *Arabidopsis*,
933 is functional in transgenic tobacco cells. Proc. Natl. Acad. Sci. 103:10104–
934 9
935 Yoshida, T., Fujita, Y., Maruyama K, Mogami, J., Todaka, D., Shinozaki, K., and
936 Yamaguchi-Shinozaki, K. 2015. Four Arabidopsis AREB/ABF transcription
937 factors function predominantly in gene expression downstream of SnRK2
938 kinases in abscisic acid signalling in response to osmotic stress. Plant, Cell
939 Environ. 38:35–49
940 Yu, X., Feng, B., He, P., and Shan, L. 2017. From Chaos to Harmony:
941 Responses and Signaling upon Microbial Pattern Recognition. Annu. Rev.
942 Phytopathol. 55:109–146
943 Yuan, M., Jiang, Z., Bi, G., Nomura, K., Liu, M., He, S., Zhou, J.-M., and Xin, X.-
944 F. 2021. Pattern-recognition receptors are required for NLR-mediated plant
945 immunity. Nature. 592:105–9
946 Zhao, C., Zayed, O., Yu, Z., Jiang, W., Zhu, P., Hsu, C., Zhang, L., Tao, W.,
947 Lozano-Duran, R., and Zhu, J. 2018. Leucine-rich repeat extensin proteins
948 regulate plant salt tolerance in Arabidopsis. Proc. Natl. Acad. Sci.
949 115:13123–28

950 Zipfel, C., Kunze, G., Chinchilla, D., Caniard, A., Jones, J. D. G., Boller, T., and
951 Felix, G. 2006. Perception of the Bacterial PAMP EF-Tu by the Receptor
952 EFR Restricts Agrobacterium-Mediated Transformation. Cell. 125:749–60
953 Zuccaro, A., Lahrmann, U., Güldener, U., Langen, G., Pfiffi, S., Biedenkopf, D.,
954 Wong, P., Samans, B., Grimm, C., Basiewicz, M., Murat, C., Martin, F., and
955 Kogel, K.-H. 2011. Endophytic Life Strategies Decoded by Genome and
956 Transcriptome Analyses of the Mutualistic Root Symbiont Piriformospora
957 indica. PLoS Pathog. 7:e1002290
958
959

960 **Figure Legends**

961

962 **Fig. 1.** PRRs confer salt stress tolerance in *Arabidopsis thaliana* following
963 recognition of cognate DAMPs. **A,** Phenotype of *A. thaliana* seedlings after (left)
964 6 days of exposure to 150 mM NaCl and (right) 5 days of exposure to 175 mM
965 NaCl, with or without Pep2 or Pep1 pretreatments. **B,** Survival rate (mean
966 ±s.e.m., n ≥ 50, 2 replicates) of seedlings after their exposure to 150 mM NaCl
967 for the indicated duration, with and without 0.1 μM Pep1 pretreatment. ***p
968 <0.001 and **p <0.01 using two-tailed t-tests compared to the corresponding
969 values of the mock-treated plants. **C,** Average fresh weights (mean ±s.e.m., n ≥
970 30, 4 replicates) of seedlings after 5 days of exposure to 150 mM NaCl, with
971 and without 0.1 μM Pep1 pretreatment. *p <0.05 using two-tailed t-tests
972 compared to the corresponding values of the mock-treated plants, N.S.- Not
973 significant. **D**, Chlorophyll contents (mean ±s.e.m., n ≥ 30, 4 replicates) in
974 seedlings after 5 days of exposure to 150 mM NaCl, with and without 0.1 μM
975 Pep1 pretreatment. The letters above bars indicate p <0.05 using Tukey's HSD
976 tests. **E,** Phenotype of seedlings after 5 days of exposure to 175 mM NaCl, with
977 or without 0.1 μM of flg22 or elf18 pretreatment. **F,** Survival rate (mean ±s.e.m.,
978 n ≥ 20, 2 replicates) of seedlings after 6 days of exposure to 175 mM NaCl, with
979 and without 0.1 μM flg22 or elf18 pretreatment. **p <0.01 using Tukey's HSD
980 tests compared to the value of mock-treated WT plants.

981

982 **Fig. 2.** Genetic requirements for PTI signaling components in PTST. Survival
983 rate (mean ±s.e.m., 3 replicates unless otherwise stated) of seedlings
984 pretreated with 0.1 μM Pep1/flg22, determined after their exposure to 175 mM
985 NaCl for the indicated durations: *bak1-4* and *bak1-5*, 9 days (n ≥ 20); *bak1-5*

bkk1-1, 8 days (n ≥ 30) ; *bik1 pbl1*, 5 days (n ≥ 25); *rbohd*, 8 days (n ≥ 30); *pmr4*, 6 days (n ≥ 30, 2 replicates). The letters above bars indicate $p < 0.05$ using Tukey's HSD tests.

Fig. 3. Recognition of bacterial MAMPs by cognate PRRs confers salt tolerance in a manner dependent on BAK1 and BIK1. **A,** Survival rate (mean ±s.e.m.) seedlings after 7 days (n ≥ 34, 3 replicates) of exposure to 150 mM NaCl, with and without 0.1 µM flg22 pretreatment. E**,** Average fresh weights (mean ±s.e.m., n ≥ 10, 3 replicates) of seedlings after 7 days of exposure to 150 mM NaCl, with and without 0.1 µM flg22 pretreatment. **C,** Chlorophyll contents (mean ±s.e.m., n ≥ 10, 3 replicates) in seedlings after 7 days of exposure to 150 mM NaCl, with and without 0.1 µM flg22 pretreatment. The letters above bars indicate $p < 0.05$ using Tukey's HSD tests.

Fig. 4. Endogenous PROPEP-PEPR signaling is activated under salt stress. **A,** Live cell imaging of *pPROPEP3*::*PROPEP3-VENUS* in *A. thaliana* roots under 150 mM NaCl for 24 h. **B,** Immunoblot analysis for extracellular fractions (growth media) of PROPEP3-VENUS seedlings exposed to 0.5 µM Pep1, 150 mM NaCl or combinations thereof. Positions of the molecular mass markers shown on the left. Experiments were repeated twice with the same conclusions. **C,** Survival rate (mean ± s.e.m, n ≥20, 2 replicates) of seedlings after 4 days of exposure to 175 mM NaCl, without MAMP/DAMP pretreatment. $^{**}p < 0.01$ and $^{*}p < 0.05$ using Tukey's HSD compared to the values of *pepr1 pepr2* plants. **D,** Chlorophyll contents (mean ±s.e.m., 4 replicates) in seedlings after 14 days of exposure to 750 mM sorbitol following 7 days of pretreatment with 100 mM NaCl. $^{**}p < 0.01$ using Tukey's HSD tests.

Fig. 5. Rapid and heightened activation of salt-induced transcriptional reprogramming during PTST. **A,** Scheme of PTST assay for RNA sequencing analysis. **B,** Number of Pep1- and/or salt-induced DEGs after exposure of seedlings to 150 mM NaCl for the indicated durations. **C,** Venn diagram illustrating the overlap between elf18-, Pep2-, salt- and Pep1-PTST-inducible DEGs. Numerals represent the numbers of the genes. **D,** A heatmap depicting salt-DEGs and Pep1-PTST DEGs using one minus Pearson correlation complete linkage hierarchical clustering. **E**, *Cis*-element enrichment analysis with CentriMo for the regulatory DNA sequences within 1-kb (from 500 corresponding to the transcription starting sites to -500 on the X-axis) upstream of 343 genes in the Cluster 5, whose salt-induction was sensitized following Pep1 pretreatment. The results for the most over-represented 4 transcription factors are shown. **F**, Immunoblot analysis for 9-day-old seedlings exposed to 175 mM NaCl for the indicated times following 0.1 μM Pep1 pretreatment. Positions of the molecular weight markers (left) and Ponceau S-stained loading controls (bottom) are shown. Experiments were repeated three times with the same conclusions. Numerals below the immunoblots indicate the band intensities relative to that of the corresponding loading control in the representative blots.

Fig. 6. Non-pathogenic bacteria confer salt tolerance through the host PRRs and PTI signaling components. **A,** Survival rate (mean ± s.e.m., n ≥ 25, 3 replicates) of WT seedlings after 5 days of exposure to 175 mM NaCl following preinoculation with the indicated *Pst* DC3000 strains. ** p <0.01 using Tukey's HSD tests compared to the values of the mock control. **B**-**E,** Survival rate

(mean ± s.e.m., n ≥ 20, 3 replicates in C-E, and 4 replicates in B) of seedlings exposed to 175 mM NaCl for 5 days in B-D, and 4 days in E following inoculation with the indicated live or dead bacteria. HK-*Pfo:* heat-killed *Pfo*. ***p* < 0.01 and **p* < 0.05 using Tukey's HSD tests compared to the values of mock-treated WT plants.

Fig.7. A model for PRR signaling cascade during PTST. Following the recognition of cognate MAMP/DAMP ligands, PRRs trigger signaling cascades through previously described PRR complexes and signaling regulators, which lead to primed and rapid activation of the salt-adaptive transcriptome during PTST, summarized in a Venn diagram based on the transcriptome profiles in Fig. 5C. Our findings propose that DAMPs from cellular damage and MAMPs from plant-associated microbes under salt stress involve PRRs in signaling toward salt stress tolerance. Dotted lines indicate the actions/links hypothesized.

Table 1. PEPR1 and PEPR2 both contribute to Pep-induced salt tolerance in *A. thaliana*.
Survival rate (%) of seedlings 7 days after exposure to 175 mM NaCl.

Genotype	Pretreatment	Survivors	Total seedlings	Survival rate (%)	Fisher's test (vs WT)	Fisher's test (vs mock)
WT	Mock	5	30	16.6		
	Pep1	29	30	96.7		p <0.01
	Pep3	30	46	65.2		p <0.01
	Pep4	40	50	80		p <0.01
	Mock	6	136	4.4		
	Pep2	87	140	62.1		p <0.01
pepr1	Mock	5	35	14.3		
	Pep1	26	30	86.7	N.S.	p <0.01
pepr2	Mock	1	30	3.3		
	Pep1	30	30	100	N.S.	p <0.01

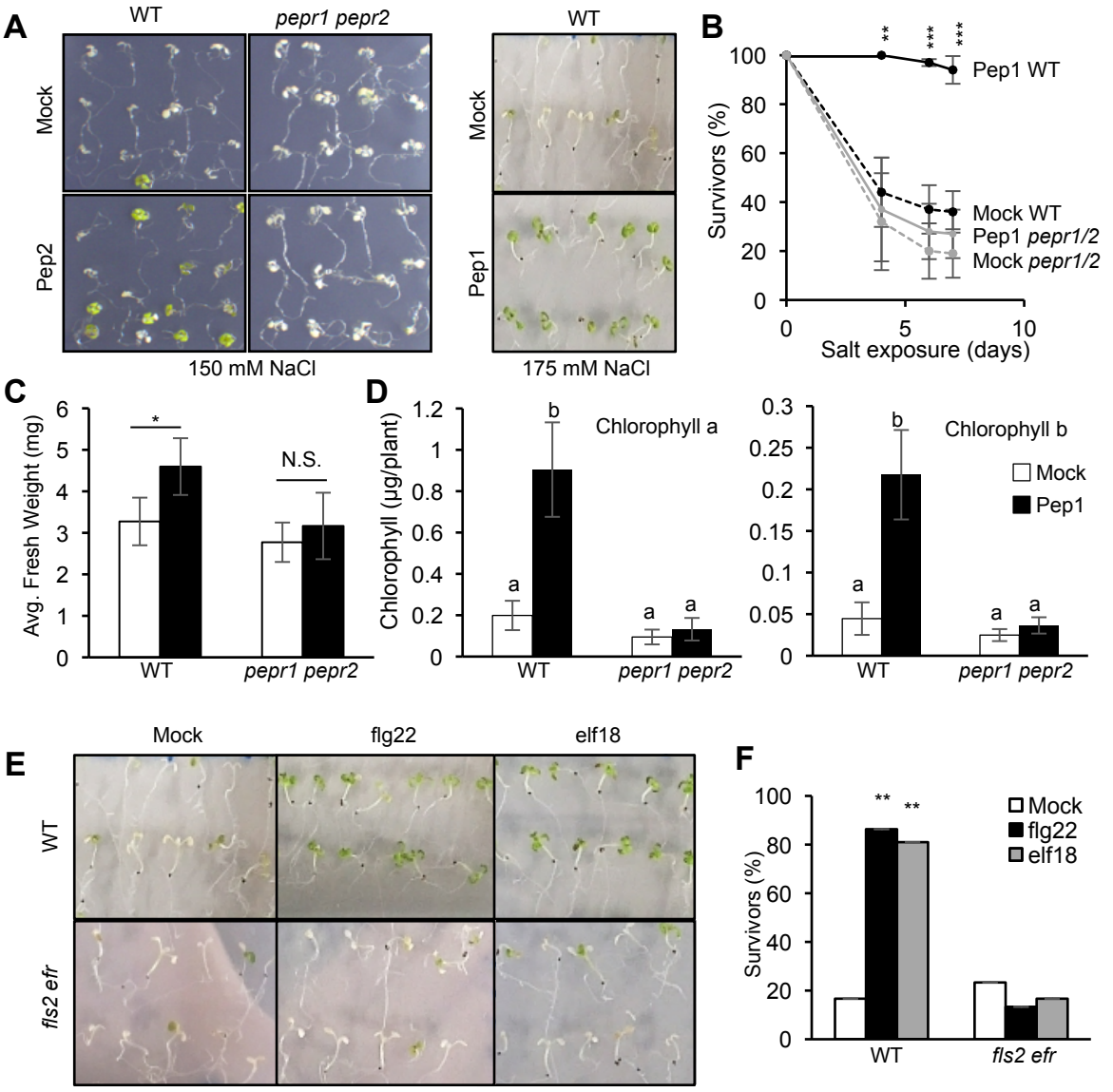

Fig. 1. PRRs confer salt stress tolerance in *Arabidopsis thaliana* following recognition of cognate DAMPs. **A,** Phenotype of *A. thaliana* seedlings after (left) 6 days of exposure to 150 mM NaCl and (right) 5 days of exposure to 175 mM NaCl, with or without Pep2 or Pep1 pretreatments. **B,** Survival rate (mean ±s.e.m., n ≥ 50, 2 replicates) of seedlings after their exposure to 150 mM NaCl for the indicated duration, with and without 0.1 µM Pep1 pretreatment. ***p <0.001 and **p <0.01 using two-tailed t-tests compared to the corresponding values of the mock-treated plants. **C,** Average fresh weights (mean ±s.e.m., n ≥ 30, 4 replicates) of seedlings after 5 days of exposure to 150 mM NaCl, with and without 0.1 µM Pep1 pretreatment. *p <0.05 using two-tailed t-tests compared to the corresponding values of the mock-treated plants, N.S.- Not significant. **D**, Chlorophyll contents (mean ±s.e.m., n ≥ 30, 4 replicates) in seedlings after 5 days of exposure to 150 mM NaCl, with and without 0.1 µM Pep1 pretreatment. The letters above bars indicate p <0.05 using Tukey's HSD tests. **E,** Phenotype of seedlings after 5 days of exposure to 175 mM NaCl, with or without 0.1 µM of flg22 or elf18 pretreatment. **F,** Survival rate (mean ±s.e.m., n ≥ 20, 2 replicates) of seedlings after 6 days of exposure to 175 mM NaCl, with and without 0.1 µM flg22 or elf18 pretreatment. **p <0.01 using Tukey's HSD tests compared to the value of mock-treated WT plants.

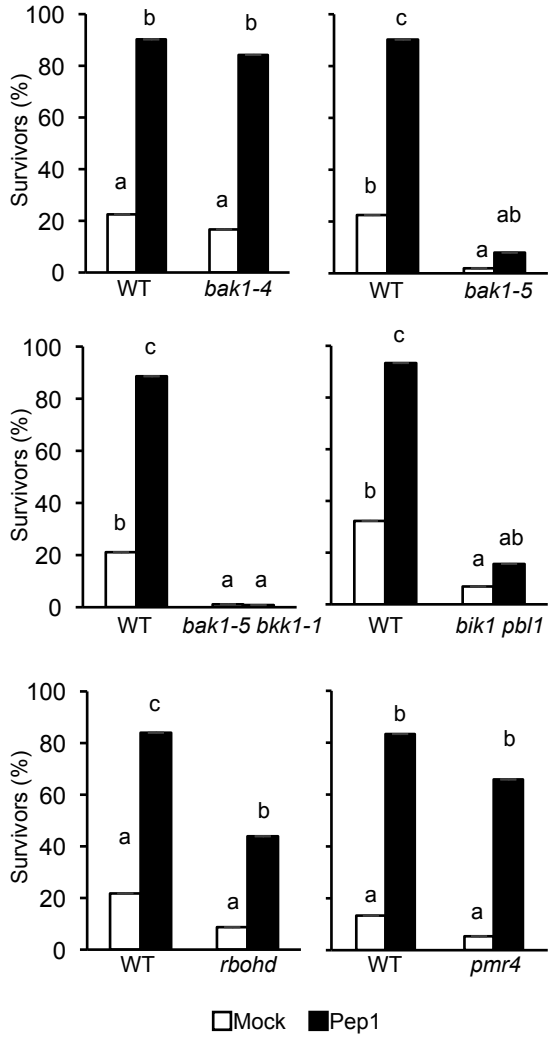

Fig. 2. Genetic requirements for PTI signaling components in PTST. Survival rate (mean ±s.e.m., 3 replicates unless otherwise stated) of seedlings pretreated with 0.1 μM Pep1/flg22, determined after their exposure to 175 mM NaCl for the indicated durations: *bak1-4* and *bak1-5*, 9 days (n ≥ 20); *bak1-5 bkk1-1*, 8 days (n ≥ 30) ; *bik1 pbl1*, 5 days (n ≥ 25); *rbohd*, 8 days (n ≥ 30); *pmr4*, 6 days (n ≥ 30, 2 replicates). The letters above bars indicate $p < 0.05$ using Tukey's HSD tests.

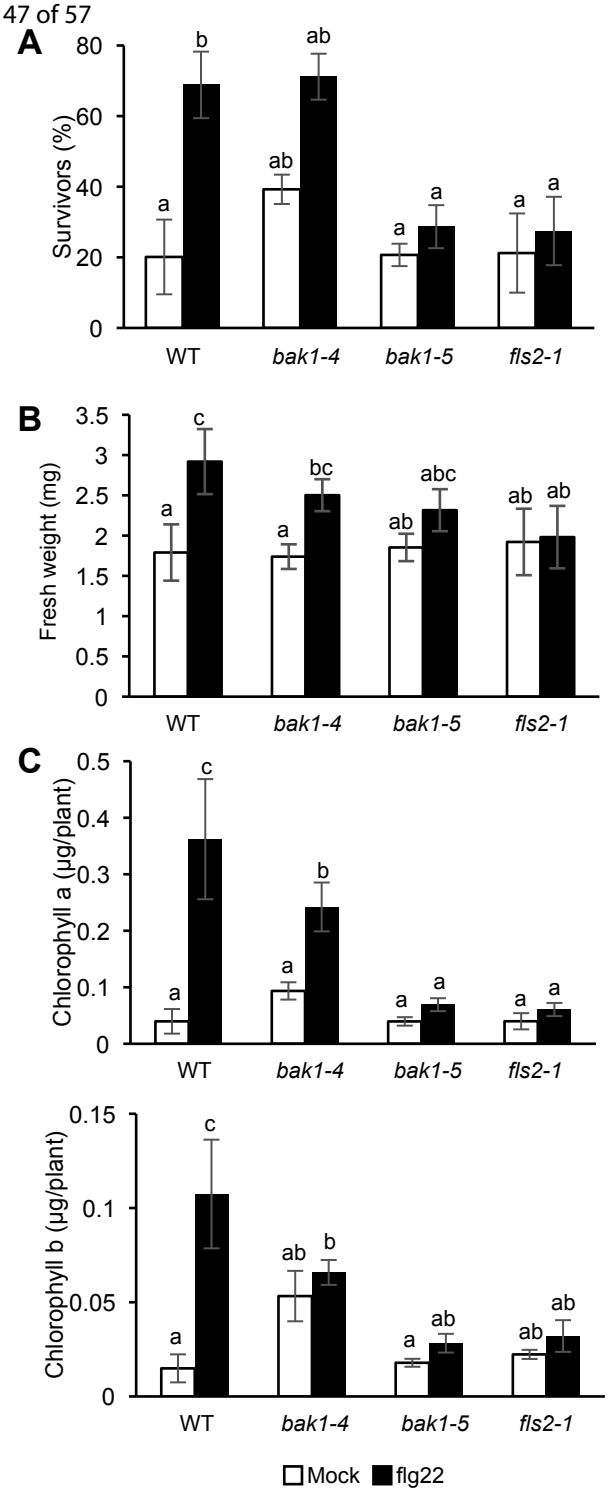

Fig. 3. Recognition of bacterial MAMPs by cognate PRRs confers salt tolerance in a manner dependent on BAK1 and BIK1. **A,** Survival rate (mean ±s.e.m.) seedlings after 7 days (n ≥ 34, 3 replicates) of exposure to 150 mM NaCl, with and without 0.1 µM flg22 pretreatment. E**,** Average fresh weights (mean ±s.e.m., n ≥ 10, 3 replicates) of seedlings after 7 days of exposure to 150 mM NaCl, with and without 0.1 µM flg22 pretreatment. **C,** Chlorophyll contents (mean ±s.e.m., n ≥ 10, 3 replicates) in seedlings after 7 days of exposure to 150 mM NaCl, with and without 0.1 µM flg22 pretreatment. The letters above bars indicate p <0.05 using Tukey's HSD tests.

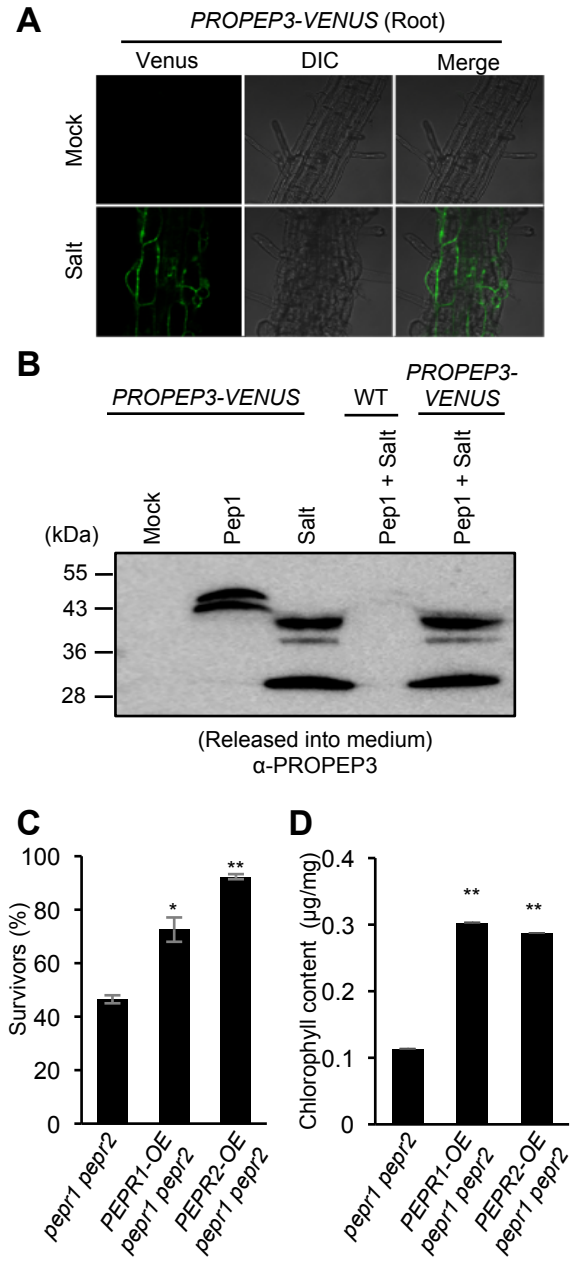

Fig. 4. Endogenous PROPEP-PEPR signaling is activated under salt stress. **A,** Live cell imaging of *pPROPEP3*::*PROPEP3-VENUS* in *A. thaliana* roots under 150 mM NaCl for 24 h. **B,** Immunoblot analysis for extracellular fractions (growth media) of PROPEP3-VENUS seedlings exposed to 0.5 µM Pep1, 150 mM NaCl or combinations thereof. Positions of the molecular mass markers shown on the left. Experiments were repeated twice with the same conclusions. **C,** Survival rate (mean ± s.e.m, n ≥20, 2 replicates) of seedlings after 4 days of exposure to 175 mM NaCl, without MAMP/DAMP pretreatment. $^{**}p$ <0.01 and $^{*}p$ <0.05 using Tukey's HSD compared to the values of *pepr1 pepr2* plants. **D,** Chlorophyll contents (mean ±s.e.m., 4 replicates) in seedlings after 14 days of exposure to 750 mM sorbitol following 7 days of pretreatment with 100 mM NaCl. $^{**}p$ <0.01 using Tukey's HSD tests.

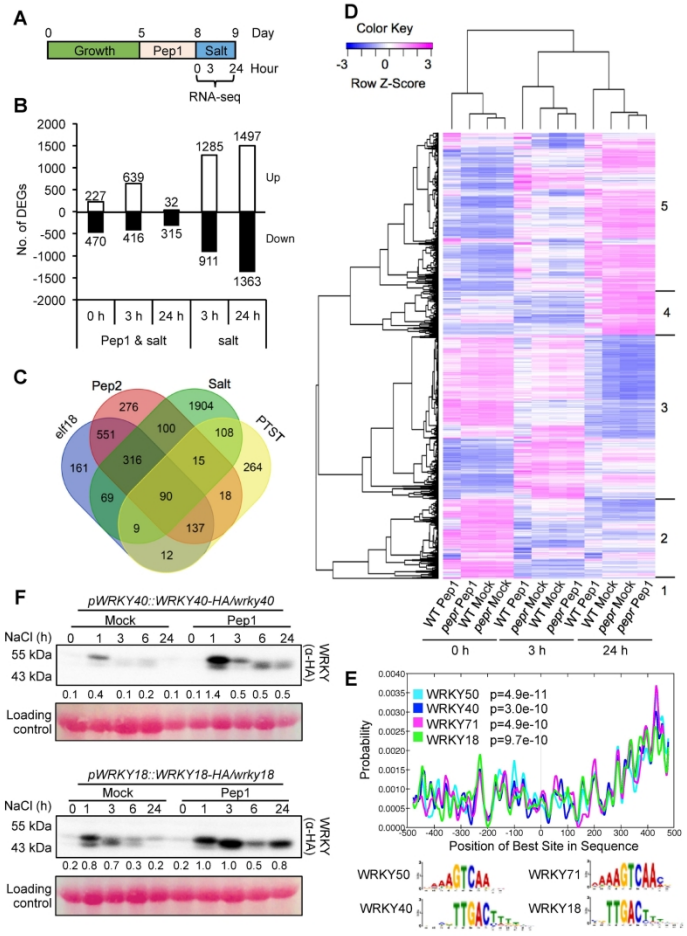

Fig. 5. Rapid and heightened activation of salt-induced transcriptional reprogramming during PTST. A, Scheme of PTST assay for RNA sequencing analysis. B, Number of Pep1- and/or salt-induced DEGs after exposure of seedlings to 150 mM NaCl for the indicated durations. C, Venn diagram illustrating the overlap between elf18-, Pep2-, salt- and Pep1-PTST-inducible DEGs. Numerals represent the numbers of the genes. D, A heatmap depicting salt-DEGs and Pep1-PTST DEGs using one minus Pearson correlation complete linkage hierarchical clustering. E,Cis-element enrichment analysis with CentriMo for the regulatory DNA sequences within 1-kb (from 500 corresponding to the transcription starting sites to -500 on the X-axis) upstream of 343 genes in the Cluster 5, whose salt-induction was sensitized following Pep1 pretreatment. The results for the most over-represented 4 transcription factors are shown. F, Immunoblot analysis for 9-day-old seedlings exposed to 175 mM NaCl for the indicated times following 0.1 μM Pep1 pretreatment. Positions of the molecular weight markers (left) and Ponceau S-stained loading controls (bottom) are shown. Experiments were repeated three times with the same conclusions. Numerals below the immunoblots indicate the band intensities relative to that of the corresponding loading control in the representative blots.

209x296mm (300 x 300 DPI)

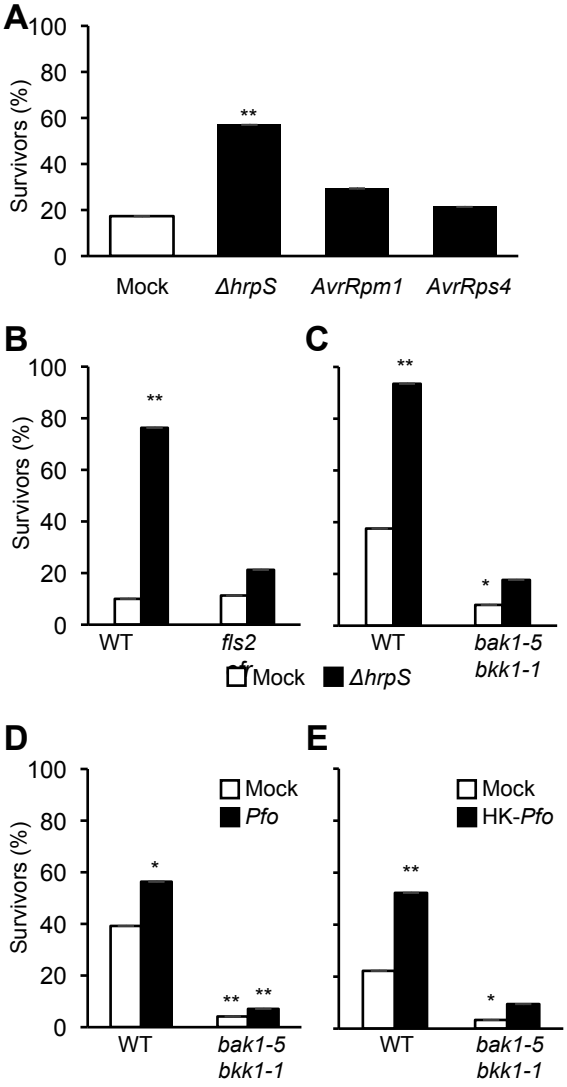

Fig. 6. Non-pathogenic bacteria confer salt tolerance through the host PRRs and PTI signaling components. **A,** Survival rate (mean ± s.e.m., n ≥ 25, 3 replicates) of WT seedlings after 5 days of exposure to 175 mM NaCl following preinoculation with the indicated *Pst* DC3000 strains. ***p* <0.01 using Tukey's HSD tests compared to the values of the mock control. **B**-**E,** Survival rate (mean ± s.e.m., n ≥ 20, 3 replicates in C-E, and 4 replicates in B) of seedlings exposed to 175 mM NaCl for 5 days in B-D, and 4 days in E following inoculation with the indicated live or dead bacteria. HK-*Pfo:* heat-killed *Pfo.* ***p* < 0.01 and **p* < 0.05 using Tukey's HSD tests compared to the values of mock-treated WT plants.

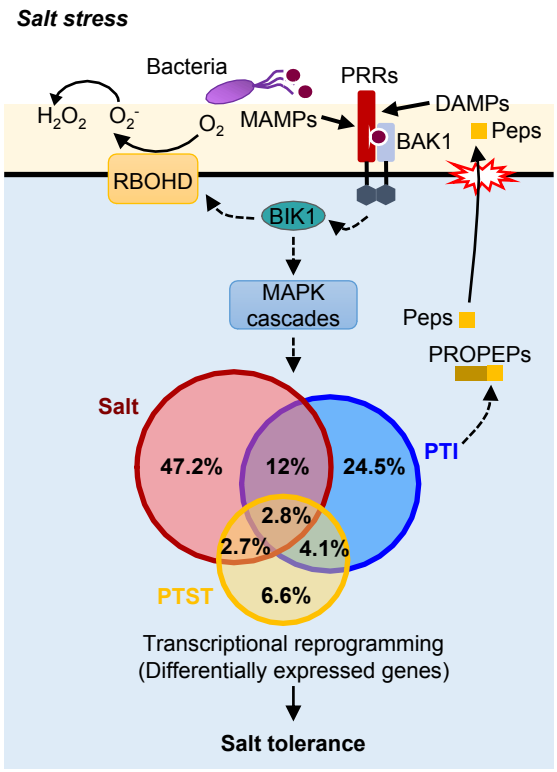

Fig.7. A model for PRR signaling cascade during PTST. Following the recognition of cognate MAMP/DAMP ligands, PRRs trigger signaling cascades through previously described PRR complexes and signaling regulators, which lead to primed and rapid activation of the salt-adaptive transcriptome during PTST, summarized in a Venn diagram based on the transcriptome profiles in Fig. 5C. Our findings propose that DAMPs from cellular damage and MAMPs from plant-associated microbes under salt stress involve PRRs in signaling toward salt stress tolerance. Dotted lines indicate the actions/links hypothesized.

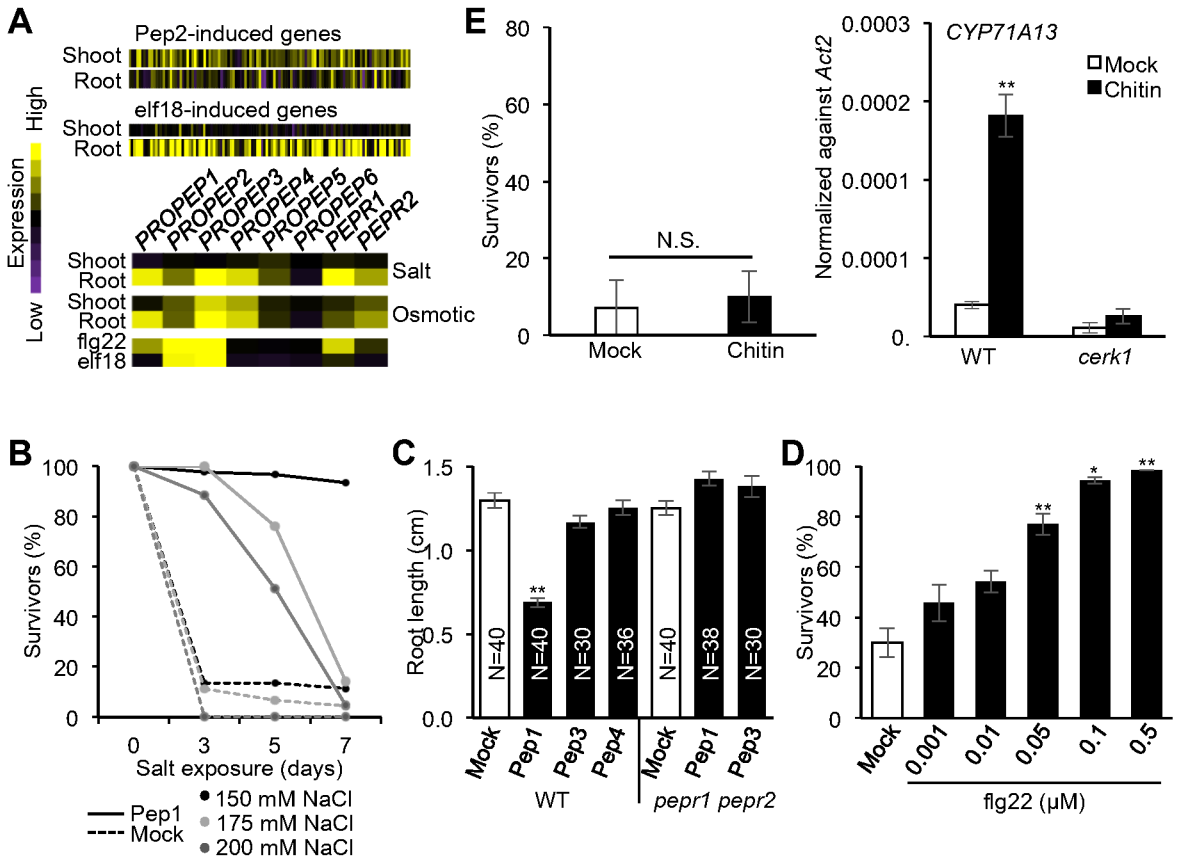

Supplementary Fig. S1. Effects of MAMP/DAMP on salt stress responses in *A. thaliana*. **A,** *In silico* expression analysis for the top 1000 Pep2- and elf18-inducible genes in the roots and shoots under salt stress, and for *PROPEP* and *PEPR* genes under the indicated conditions. Analyses performed with Genevestigator databases AT-00597 (elf18 and Pep2), AT-00120 (salt, osmotic). **B,** Survival rate (mean ±s.e.m., n ≥40, 2 replicates, for 175 mM NaCl, n >40, 1 replicate) of WT seedlings after indicated duration of exposure to 150-200 mM NaCl, with and without 0.1 μM Pep1 pretreatment. **C,** Root lengths (mean ±s.e.m., n ≥ 30) of *A. thaliana* seedlings exposed to 0.1 μM Pep1, Pep3 or Pep4 for 4 days. **D,** Survival rate (mean ±s.e.m., n ≥ 35, 2 replicates) of WT seedlings 7 days after exposure to 175 mM NaCl following flg22 pretreatment at the indicated doses.. **E**, (left) Survival rate (mean ±s.e.m., n ≥30, 2 replicates) of WT seedlings after 7 days of exposure to 175 mM NaCl following 100 μg/ml chitin pretreatment, and (right) qRT-PCR analysis for *CYP71A13* in 7-day-old seedlings treated with 100 μg/ml chitin for 1 h. Data represent mean ± s.e.m., n = 3. For B-E, **, $p < 0.01$ using Tukey's HSD compared to the value of mock-treated WT, N.S.- not significant using two-tailed t-test.

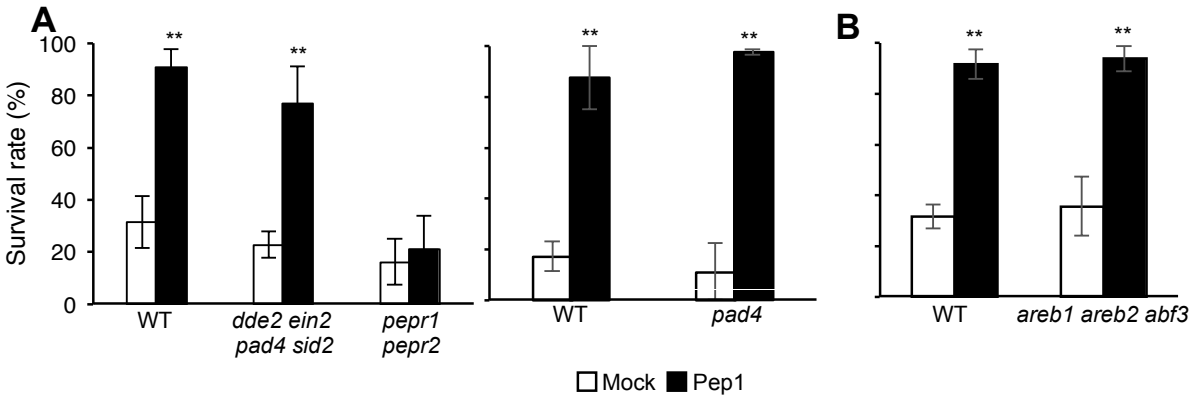

C

Genotype	Pretreatment	Survivors	Total seedlings	Survival rate (%)	Fisher's test (vs WT)	Fisher's test (vs mock)
WT	Mock	3	54	5.6		
	Pep2	48	57	84.2		p <0.01
aba2-12	Mock	1	61	1.6	N.S.	
	Pep2	44	61	72.1	N.S.	p <0.01

Supplementary Fig. S2. Defense-related phytohormones and ABA are dispensable in PTST. **A-C,** Survival rate (mean ± s.e.m.) of seedlings after exposure to 175 mM NaCl for the indicated duration following 0.1 μM Pep1/Pep2 pretreatment. *dde2 ein2 pad4 sid2*, 4 days (n ≥33, 3 replicates); *pad4*, 6 days (n ≥ 30, 3 replicates); *areb1 areb2 abf3,* 7 days (n ≥ 38, 3 replicates); *aba-12*, 4 days. *p <0.05 and **p <0.01 using Tukey's HSD compared to the corresponding mock-treated WT values.

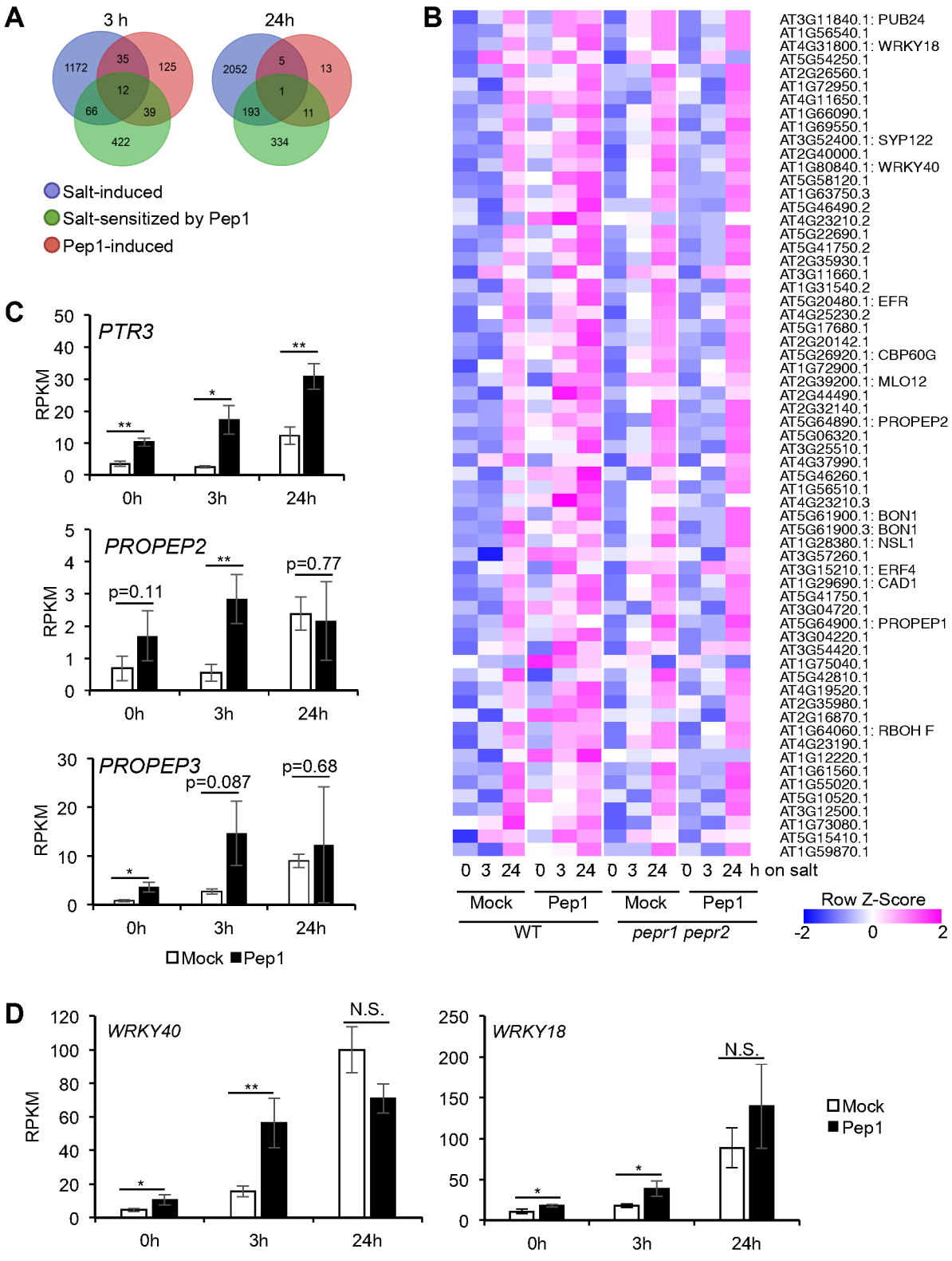
A
3 h
24h
1172
35
125
12
66
39
422
2052
5
13
1
193
11
334
Salt-induced
Salt-sensitized by Pep1
Pep1-induced
B
AT3G11840.1: PUB24
AT1G56540.1
AT4G31800.1: WRKY18
AT5G54250.1
AT2G26560.1
AT1G72950.1
AT4G11650.1
AT1G66090.1
AT1G69550.1
AT3G52400.1: SYP122
AT2G40000.1
AT1G80840.1: WRKY40
AT5G58120.1
AT1G63750.3
AT5G46490.2
AT4G23210.2
AT5G22690.1
AT5G41750.2
AT2G35930.1
AT3G11660.1
AT1G31540.2
AT5G20480.1: EFR
AT4G25230.2
AT5G17680.1
AT2G20142.1
AT5G26920.1: CBP60G
AT1G72900.1
AT2G39200.1: MLO12
AT2G44490.1
AT2G32140.1
AT5G64890.1: PROPEP2
AT5G06320.1
AT3G25510.1
AT4G37990.1
AT5G46260.1
AT1G56510.1
AT4G23210.3
AT5G61900.1: BON1
AT5G61900.3: BON1
AT1G28380.1: NSL1
AT3G57260.1
AT3G15210.1: ERF4
AT1G29690.1: CAD1
AT5G41750.1
AT3G04720.1
AT5G64900.1: PROPEP1
AT3G04220.1
AT3G54420.1
AT1G75040.1
AT5G42810.1
AT4G19520.1
AT2G35980.1
AT2G16870.1
AT1G64060.1: RBOH F
AT4G23190.1
AT1G12220.1
AT1G61560.1
AT1G55020.1
AT5G10520.1
AT3G12500.1
AT1G73080.1
AT5G15410.1
AT1G59870.1
0 3 24 0 3 24 0 3 24 0 3 24 h on salt
Mock
Pep1
Mock
Pep1
WT
pepr1 pepr2
Row Z-Score
-2
0
2
C
PTR3
RPKM
50
40
30
20
10
0
**
*
**
0h
3h
24h
PROPEP2
RPKM
5
4
3
2
1
0
p=0.11
**
p=0.77
0h
3h
24h
PROPEP3
RPKM
30
20
10
0
p=0.087
p=0.68
*
0h
3h
24h
Mock
Pep1
D
WRKY40
RPKM
120
100
80
60
40
20
0
*
**
N.S.
0h
3h
24h
WRKY18
250
200
150
100
50
0
*
*
N.S.
0h
3h
24h
Mock
Pep1

Supplementary Fig. S3. Rapid activation and expansion of salt-adaptive transcriptome during PTST. **A,** Venn diagram illustrating the overlap among salt-inducible DEGs (WT mock, salt for 0 h < 3 h/24 h), Pep1-inducible DEGs (WT mock < WT Pep1 for 3 d), and salt-sensitized genes after Pep1 pretreatment ([WT Pep1 salt 0 h < 3 h/24 h] & [WT mock salt 3 h/24 h < WT Pep1 salt 3 h/24 h]. Left, salt 3 h; Right: salt 24 h. (**B**) A heatmap illustrating 343 genes in cluster 5, whose salt-induction hastened following Pep1 pretreatment. Analyses performed using one minus Pearson correlation complete linkage hierarchical clustering **C,** Gene expression levels (mean ± s.d.) for the indicated genes extracted from the transcriptome data used in Figure 5. *p <0.05 and **p <0.01 using student's t-test compared to the values of the corresponding mock controls. N.S.- Not Significant. **D,** Gene expression levels (mean ± s.d.) for the indicated genes extracted from the transcriptome data used in Figure 5. *p <0.05 and **p <0.01 using Student's t-test compared to the values of the corresponding mock controls. N.S.- Not Significant.

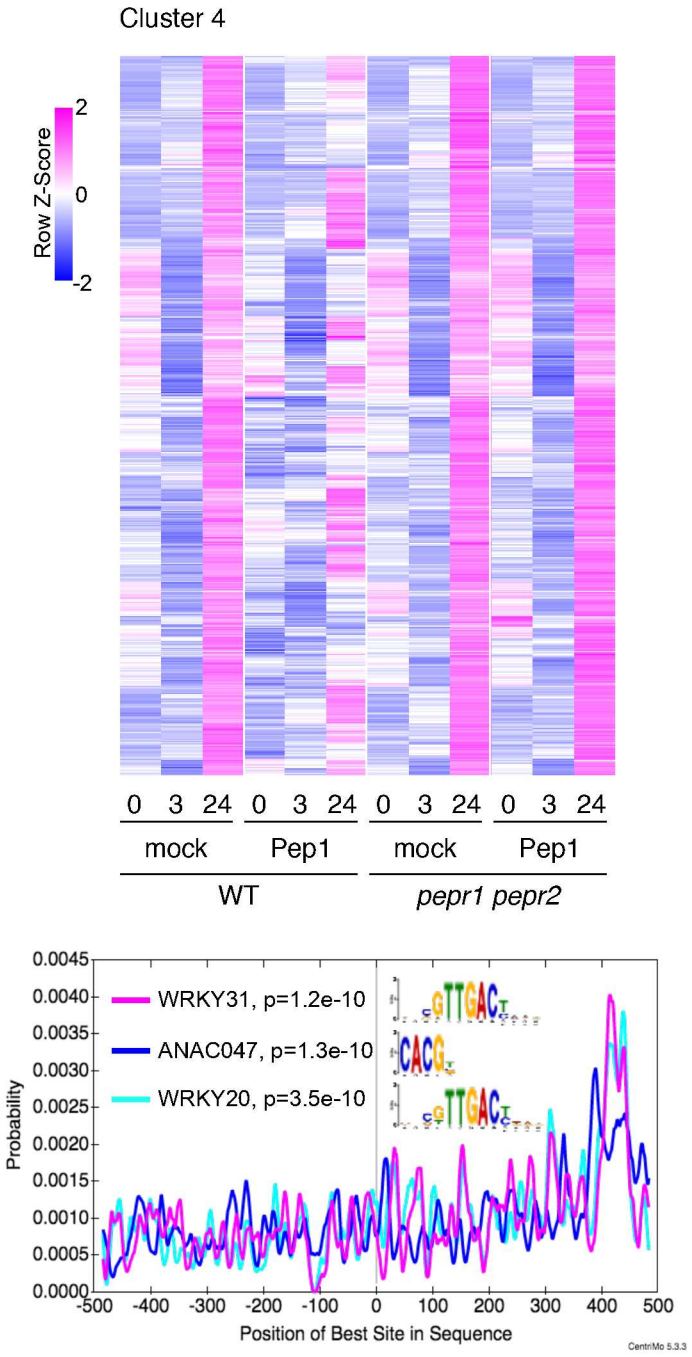

Supplementary Fig. S4. A subset of salt-inducible genes suppressed by Pep1 during PTST. A heatmap illustrating genes in cluster 4, whose salt-induction is suppressed following Pep1 pretreatment. Analyses performed using one minus Pearson correlation complete linkage hierarchical clustering.